MEMS mass spectrometers: the next wave of miniaturization

You may also be interested in:

A microengineered alignment bench for a nanospray ionization source
R R A Syms, H Zou, M Bardwell et al.

Quadrupole mass spectrometry of reactive plasmas
J Benedikt, A Hecimovic, D Ellerweg et al.

Progress in vacuum technology
J Pollard

Identification techniques for nuclear particles in space plasma research and selected experimental results
B Wilken

Challenges and trends in magnetic sensor integration with microfluidics for biomedical applications
S Cardoso, D C Leitao, T M Dias et al.

Gas chromatography-mass spectrometry combinations
A M Greenway and C F Simpson

DART mass spectrometry and its applications in chemical analysis
Elena S Chernetsova, G E Morlock and Igor A Revelsky

Topical Review

MEMS mass spectrometers: the next wave of miniaturization

Richard R A Syms[1] and Steven Wright[2]

[1] EEE Department, Imperial College London, Exhibition Road, London SW7 1AZ, UK
[2] Microsaic Systems, GMS House, Boundary Road, Woking, Surrey GU21 5BX, UK

E-mail: r.syms@imperial.ac.uk

Abstract
This paper reviews mass spectrometers based on micro-electro-mechanical systems (MEMS) technology. The MEMS approach to integration is first briefly described, and the difficulties of miniaturizing mass spectrometers are outlined. MEMS components for ionization and mass filtering are then reviewed, together with additional components for ion detection, vacuum pressure measurement and pumping. Mass spectrometer systems containing MEMS sub-components are then described, applications for miniaturized and portable systems are discussed, and challenges and opportunities are presented.

Keywords: mass spectrometer, mass filter, MEMS

(Some figures may appear in colour only in the online journal)

1. Introduction

Microelectromechanical systems (MEMS) technology—the use of microfabrication techniques to construct integrated systems—has had a major impact on sensors and actuators since the 1980s [1–5]. Applications have been found in the automotive, aerospace, consumer, information technology, telecommunications, defense and security, energy, and biomedical sectors. MEMS are available as commodity items or as specialized enablers for high-value instruments. Operation can involve mechanical, electrical, optical, thermal, fluidic, chemical and biochemical principles. Each requires specialized materials and processing, and device formats can be very different. Many MEMS are based on silicon-compatible materials, but metals, plastics, glasses and ceramics all have specific applications. Many different fabrication techniques have been developed, but most can only be used with particular materials. As a result, there is no universal 'roadmap' for MEMS, and development costs have often been high.

In contrast to micro-total-analysis systems (μTAS) [6–9], which were developed quickly, MEMS mass spectrometers have taken decades to reach market. For example, a patent describing an elementary MEMS mass filter that was originally filed in 1996 [10] eventually led to a considerably more complex desktop mass spectrometer in 2011 [11]. The most obvious reason is the need for a bulky vacuum system, which renders the case for miniaturizing a sub-component such as a mass filter much less convincing. Commercial reasons include low unit sales, high development cost, and a disadvantageous tradeoff between size and performance. Additional technical reasons include the confusing range of designs, the complexity of the structures needed in each case, and the poor performance of early systems. As a result, development was supported by the space and defense sectors (which have an overwhelming need for portability) for many years. However, considerable progress has recently been made. Performance has improved dramatically, markets have been identified, and commercial instruments incorporating MEMS are now available.

The aim of this paper is to describe this new success story. Approaches to miniaturizing components for mass spectrometers are first described in section 2, focusing on microfabricated

devices. MEMS embodiments of the main sub-components—ion sources, mass filters, ion detectors, vacuum gauges, and pumps—are reviewed in sections 3–5. In each case, relevant background is given, followed by a summary of achievements to date. Assembly of MEMS components into mass spectrometer systems is considered in section 6. Applications for small mass spectrometers are described in section 7 and opportunities and challenges for MEMS mass spectrometers are presented in section 8.

2. MEMS mass spectrometers

2.1. Background

Miniaturized mass spectrometers were first developed in the early 1970s for applications such as residual gas analysis (RGA) and space exploration [12–14]. There was a resurgence of interest in the 1990s, but progress was slow. Manufacturers were focused on the lucrative pharmaceutical sector, which demanded high-performance instruments for drug development, and interest was concentrated on combining chip-based separation with electrospray. Miniaturization of systems was therefore mainly driven by portable applications, an initially small market. However, in the 2000s, national security concerns rose dramatically and interest in field-deployable instruments greatly increased.

All mass spectrometers require an ion source, a mass filter, and an ion detector. However, in each case, a bewildering number of variants exist. For example, figure 1 shows the main types of mass filter: (a) the magnetic sector, (b) the crossed-field or Wien filter, (c) the Fourier transform ion cyclotron resonance (FT-ICR) mass spectrometer, (d) the time-of-flight filter, (e) the quadrupole mass spectrometer (QMS), and (f) the quadrupole ion trap (QIT) [15]. Others, such as the Orbitrap, also exist, but require more complex electrodes. Complete instruments also require a vacuum chamber, a method of sample introduction, vacuum pumps, a pressure gauge, control electronics and data acquisition, display and storage.

During the early development of miniature mass spectrometry (MS), it was not clear which variant to use, how to partition a system into sub-units, or how to package the units. As a result, most teams developed single miniaturized components for use in conventional chambers pumped by compact turbo-pumps. All the filters above have been successfully miniaturized, except the FT-ICR-MS, which requires high magnetic fields. Two approaches to miniaturization were used. The first involved taking conventional technologies such as precision machining, photo-etching and printed circuit board (PCB) fabrication to their limits, and resulted in useful, but relatively large, systems. Many of the most common mass analysers were miniaturized in this way, including magnetic sector [13, 16, 17], time-of-flight [14, 18, 19], quadrupole [20–22], cylindrical ion trap [23–25] and linear ion trap [26–28] filters. This work is described in excellent reviews [29, 30]. The second involved MEMS; however, microfabrication was in its infancy and

this approach typically yielded smaller systems, but with initially poor performance.

2.2. MEMS processes

Early MEMS technologies unfortunately proved unsuitable for fabricating most MS components. For example, bulk micromachining [31] involves etching down crystal planes in single crystal substrates using wet etchants such as KOH, and is largely restricted to features following $\langle 1\,1\,1 \rangle$ planes in Si. Using $(1\,0\,0)$ substrates, these consist of V-shaped grooves and pits with sloping sidewalls. After additional oxidation and metallization, useful structures can be made, such as the quadrupole filter shown in figure 2(a) (described in more detail in section 4.7). Here, the grooves are used to mount cylindrical electrodes and insulating spacers to form a two-substrate stack. However, further lithography and processing are difficult to carry out after etching to any depth.

Surface micromachining [32] offered much greater flexibility, allowing arbitrary features to be formed in deposited layers of polysilicon and silicon dioxide, which could each be preferentially removed. Multiple cycles of deposition and etching can be carried out, but layer thickness is limited in each case to a few microns by intrinsic stress. Again, useful systems were made using surface processing, such as the Wien filter shown in figure 2(b), which combines diaphragm-based electron and ion optics with an etched vacuum chamber (described later, in section 4.3).

However, the key difficulties of miniature mass analysers were that high selectivity needed devices with a long ion path (requiring ion optical components to be set up perpendicular to the substrate) while high sensitivity needed a large pupil (so these components must be large). Much deeper (over 100 μm) structures could be fabricated by patterning a thick photoresist layer, either using UV light for exposure or using synchrotron radiation in the LIGA (Lithographie, Galvanoforming, Abformung) process [33]. In some cases, especially microfluidics, resists such as SU-8 [34] may be used as structural materials. High-aspect-ratio metal parts can also be formed, by electroplating Ni into a resist mould. However, high cost eventually led to other preferred solutions.

Particularly, deep reactive ion etching (DRIE) allowed the formation of arbitrary features in silicon with near-vertical sidewalls [35]. The structures could be extremely deep, in some cases etched right through the wafer. In the Bosch DRIE process [36, 37], verticality was achieved using inductively coupled plasma, with alternating cycles of etching using SF_6 and passivation using C_4F_8. Bonded silicon-on-insulator (BSOI) material (a silicon device layer separated from a silicon substrate by a layer of thermal oxide) and thick deposited dielectrics allowed the fabrication of electrically insulated parts. For example figure 2(c) shows the process for fabricating one half of a cylindrical ion trap; two such structures, back-to-back, form a complete trap (section 4.7).

When combined with wafer stacking [38, 39], ion optics with integral pupils could be set up perpendicular to the wafer plane. Plug assembly of deep-etched silicon components into
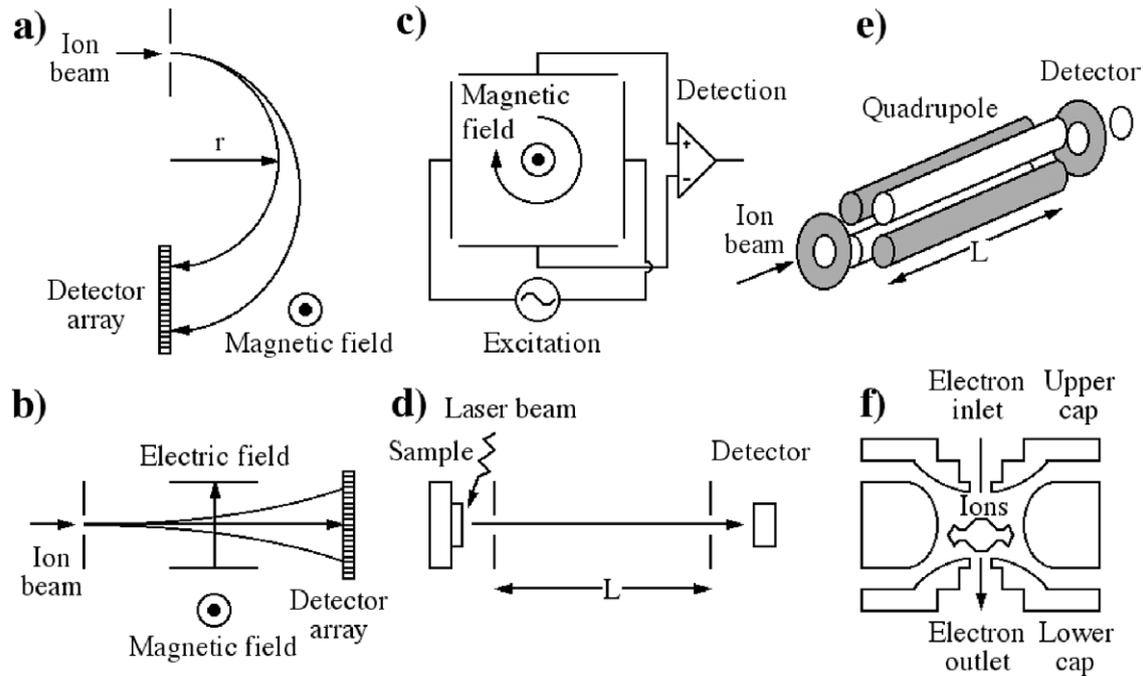
Figure 1. Mass spectrometer types: (a) magnetic sector; (b) Wien filter; (c) Fourier transform ion cyclotron resonance; (d) time of flight; (e) quadrupole filter; (f) quadrupole ion trap.

mounts containing etched silicon springs also allowed components with more general features to be fabricated flat and then assembled into a component train. Despite the advantages of BSOI, RF devices have suffered from the poor electrical isolation offered by relatively thin buried oxide layers, which typically results in heating of a semiconducting substrate. More advanced MEMS technologies such as silicon-on-glass were therefore needed to achieve a high mass-range. Other techniques that combine dissimilar materials (such as anodic bonding) have therefore also proved important.

More recently, techniques such as rapid prototyping [40, 41] have made an impact. These cannot be currently considered true MEMS technologies, but are being combined with planar processing [42] and may well have advantages in fabricating complex electrodes.

2.3. MEMS design

No new physics is required in MEMS MS. Ions are created using known methods and filtered using electric and magnetic fields, exactly as in conventional instruments. Ion dynamics can therefore be simulated by integration of the equations of motion. Nevertheless there are some differences, caused by the limitations of MEMS. These are most easily illustrated in terms of the quadrupole filter, discussed in detail in sections 4.6 and 4.7. This structure uses a hyperbolic electrostatic field $\phi(x, y) = \phi_0(x^2 - y^2)/2r_0^2$ for filtering, shown in idealized form in the left-hand inset to figure 3(a). Ions travel in the z-direction, and the potential ϕ_0 normally contains both a dc component and an RF component at angular frequency ω. Integration yields trajectories of the type shown in the main plot. Here $\zeta = \omega t$, and t is time, although with a constant axial velocity ζ is also proportional to the axial flight distance z.

The trajectory contains complex oscillations that are highly sensitive to a number of parameters including the exact shape of the field.

To reduce cost, most conventional quadrupoles are constructed using cylindrical electrodes, which approximate the desired hyperbolae. Decades of work have established the best radii and the effects of residual imperfections. However, a MEMS process of the type shown in figure 2(a) makes additional approximations by introducing grounded features in close proximity (the Si substrates). Consequently, the real field appears as shown in the right-hand inset to figure 3(a). Strenuous efforts must be made to minimize the effect of the field imperfections, since they severely limit the achievable resolution. The presence of additional features such as coupling optics (or other approximations caused by MEMS processes) then renders the overall field 3D, especially at the electrode ends. Accurate simulation is then most easily carried out numerically, for example using the commercial software SIMION®, which combines a fast field solver with a trajectory integrator [43]. Figure 3(b) shows a typical simulation of a more complex quadrupole filter constructed using BSOI, including coupling optics.

2.4. Advantages of MEMS

Earlier reviews of the application of MEMS to mass spectrometry can be found in [44–47]. Its potential advantages can be established from the limitations of conventional systems. Removing the covers from modern instruments reveals that these are very complex. The vacuum system dominates but intricate wiring looms and major subsystems responsible for high voltage dc and RF supply, pump control, gas flow control and power distribution can also be seen. Within the vacuum

chamber, an array of anchor points and ceramic stand-offs support precisely manufactured ion optical assemblies. Electrical connections are made through stiff copper wire and vacuum feed-throughs. The labour costs of assembly, testing and servicing are considerable.

A key advantage of MEMS is therefore the potential for a consumer electronics model for product integration. It is now possible to envisage that MS sub-systems or even complete systems could be manufactured on a wafer scale and assembled on PCBs, with defective systems being rejected rather than re-worked. In addition, a consequence of favourable scaling laws is that MEMS ion sources, filters and detectors can be operated at much lower voltages than their conventional counterparts. A major obstacle is the provision of vacuum, since high vacuum pumps are a major contributor to system size and cost. Fortunately, it seems that the higher pressure-tolerance of MEMS mass filters and the improving capabilities of MEMS vacuum pumps may converge. It is important that performance, particularly sensitivity, is not significantly compromised by miniaturization. Arrays of MEMS sources, filters and detectors retain the benefits of low-voltage, high-pressure operation, but increase the ion flux that can be processed.

3. MEMS ion sources and sample introduction methods

3.1. Background

A wide variety of ion sources exists; for a review, see [48]. The earliest common method is electron ionization (EI), using a heated filament as an electron source and confining electrodes to increase the likelihood of impact. The current density J obtained in an electric field E at absolute temperature T obeys the Richardson–Dushman equation $J = AT^2 \exp\{-(\phi - \Delta\phi)/k_BT\}$. Here, ϕ is the work function of the filament, k_B is Boltzmann's constant and $A = 4\pi m_e k_B^2 e/h^3$, where e and m_e are the electron charge and mass and h is Planck's constant. The field-induced term is $\Delta\phi = (eE/4\pi\varepsilon_0)^{1/2}$, where ε_0 is the vacuum permittivity. Emission will occur as soon as $\Delta\phi > \phi$, (which requires materials with low work functions) and the current will be high if T is also high (which requires filament materials that can also easily be heated, such as tungsten). However, if the field is high enough, significant emission will be obtained even at room temperature (so-called 'cold cathode' emission) [49]. High fields can be achieved using pointed (Spindt) emitters.

Later methods include flame ionization, corona discharge and inductively coupled plasma (ICP) ionization [50]. Optical methods include photo-ionization (PI) using an ultraviolet lamp [51], laser desorption ionization (LDI) [52], and its surface-enhanced and matrix-assisted variants SELDI and MALDI [53]. The most common ionization method for liquids is electrospray ionization (ESI) [54, 55]. A voltage is applied between a liquid in a capillary and a counter-electrode, and the electric field distorts the liquid surface into a Taylor cone from which charged droplets are emitted [56]. The charge density of a free droplet increases as solvent evaporates and its diameter decreases. This continues until electrostatic repulsion exceeds
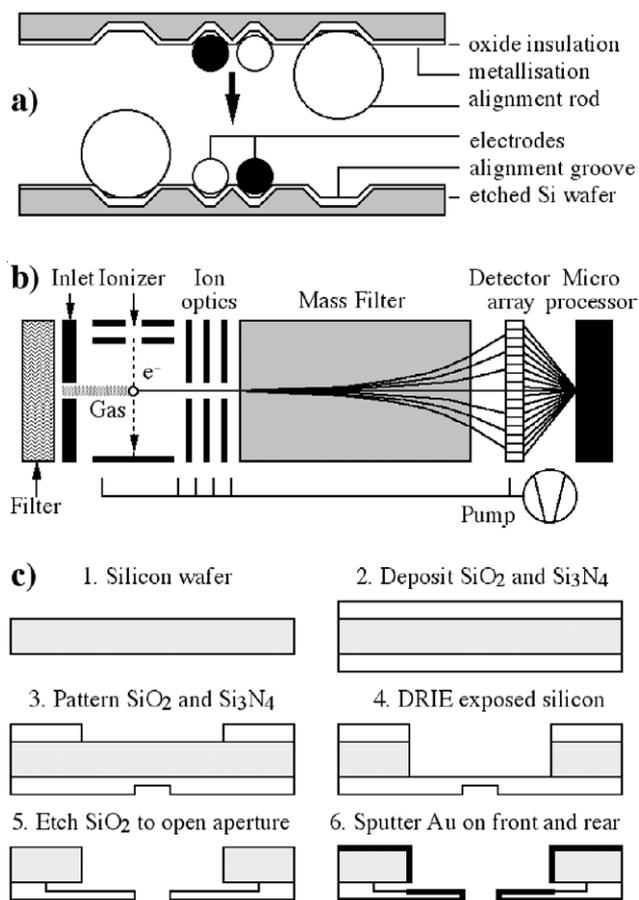

Figure 2. MS components fabricated using different MEMS processes: (a) bulk micro-machined quadrupole filter (reproduced by permission of the Institute of Engineering and Technology from Syms R R A *et al* 1996 *Elect. Lett.* **32** 2094–5 [138]); (b) surface micromachined Wien filter (reproduced by permission from Friedhoff C B *et al* 1999 *J. Vac. Sci. Technol.* A **17** 2300–7 [117], copyright JVST 1999, American Vacuum Society); (c) deep reactive ion etched cylindrical ion trap (one half thereof) (from van Amerom F H W *et al* 2007 *Chem. Eng. Commun.* **195** 98–114 [153] (© Taylor and Francis, 2007)). Reprinted with permission of the publisher (Taylor & Francis Ltd, http://www.tandfonline.com).

surface tension and the droplet undergoes fission, eventually leading to single ions (which can be multiply charged). Electrospray is carried out with capillaries of ≈100 μm internal diameter (ID), and voltages of 2.5–4 kV. Voltages are reduced in nanospray systems with capillaries of ≈10 μm ID [57, 58]. A variant—desorption electrospray ionization (DESI), in which adsorbed molecules are ionized using an electrosprayed liquid—has found wide application in surface sampling [59].

Regardless of how ionization is achieved, a means of transferring an analyte or an ion stream into vacuum is required. For gases, a needle valve or conductance-limiting capillary may suffice. For ion traps, which operate cyclically, actively pulsed, discontinuous inlets may be used to overcome pumping speed limitations [60]. A simple manual method is solid phase microextraction (SPME) [61]. This involves extraction of analytes from gas or liquid samples using a polymer-coated silica fibre, which is injected through a septum and into the chamber, where the analytes desorb. Membrane introduction allows continuous selective transfer of analytes from the gas or
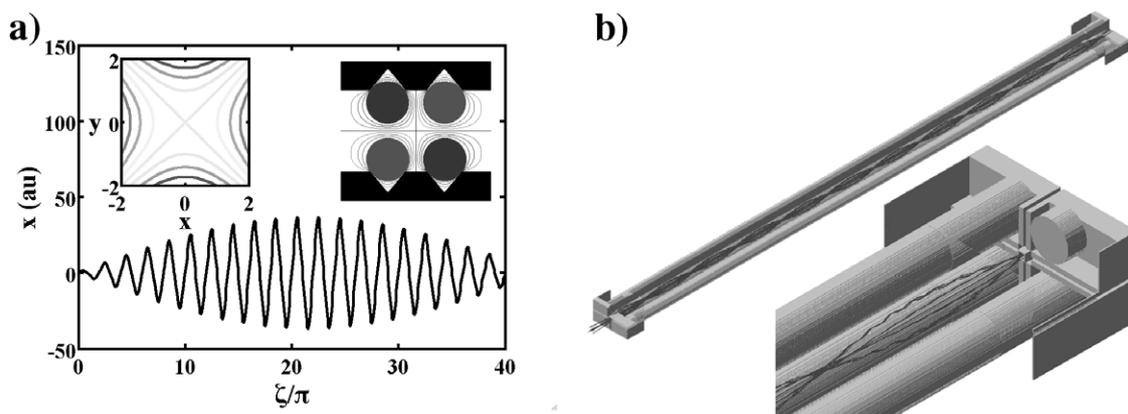
Figure 3. Modelling of MEMS MS systems: (a) Exact and approximate fields in a V-groove quadrupole filter, and example ion trajectory; (b) realistic simulation of a BSOI type quadrupole filter using SIMION® (courtesy Microsaic Systems).
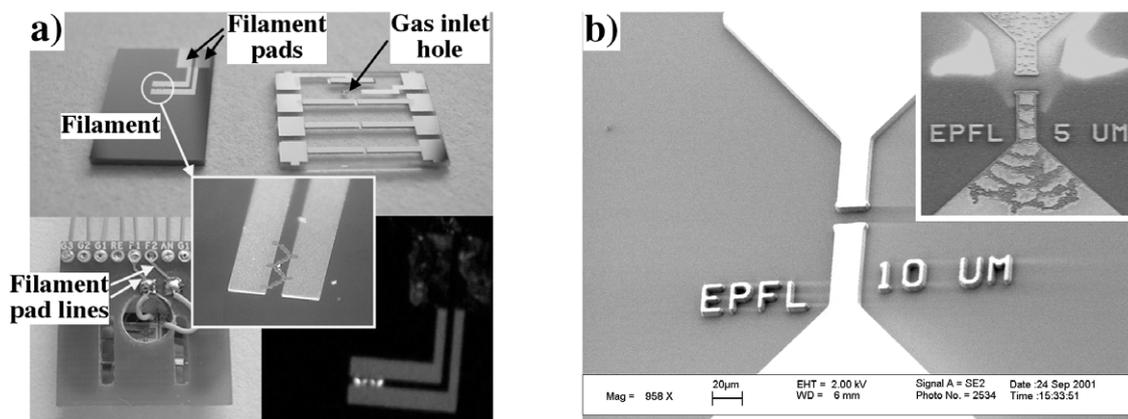

Figure 4. Microfabricated ion sources: (a) hot cathode EI source [67] (courtesy Professor Hyeun Joong Yoon, South Dakota State University; © 2007 IOP Publishing. Reproduced with permission. All rights reserved.); (b) electrodes for plasma discharge ion source, before and after prolonged use (courtesy Dr Ralph Longwitz, EPFL).

liquid phase through a porous barrier [62]. The jet expansion interface [63] is the most versatile introduction method for ions created at atmospheric pressure. In ESI-MS, other components such as air amplifiers use the Venturi effect to increase ion density in the spray [64]. Similarly, tapered arrays of ring electrodes driven by RF voltages and known as ion funnels are used to improve the coupling of ions into the inlet [65].

3.2. MEMS ion sources

Planar hot-cathode EI sources using microfabricated filaments have been demonstrated [66, 67]. Figure 4(a) shows a suspended tungsten filament for a miniature TOF mass spectrometer, with a zig-zag layout. However, integrated filaments are used relatively rarely because of their high power consumption, high temperature and the potential for thermal runaway. For this reason, more recent demonstrations have used replaceable external filaments [68]. Cold-cathode EI sources are much more common; the ability of isotropic plasma etching to form extremely sharp tips in silicon (which may easily be combined with concentric anodes) allows the high fields needed for electron emission at room temperature to be provided at low voltage [69]. Emission can also be enhanced, by over-coating with low-work function materials such as thin-film diamond [70]. The

sources are small, and can be formed in large arrays. Several small mass spectrometers with field emission sources have been constructed [71, 72], including the miniature ion trap for the European Space Agency's Rosetta Comet Rendezvous Mission [73]. More recent devices have used carbon nanoparticles [74] and nanotubes [75, 76] as sharp emitting tips, with advanced devices being fabricated in arrays with double gates [77].

No microfabricated photoionization (PI) sources have been developed, since these would require optoelectronic materials, but portable mass spectrometers employing external lasers have been demonstrated [78], and systems have been developed for combining photoionization with chip or capillary flow systems [79, 80]. Microfabricated plasma sources only require a sealed, etched chamber containing channels for gas flow and electrodes for plasma excitation, and a variety have been demonstrated using inductive and capacitive excitation [81–85] and even integrated with mass spectrometers [86]. Here, the main difficulty has been to prolong the life of the electrodes, since the relatively thin metal layers formed using most deposition methods are rapidly eroded by sputtering. For example, figure 4(b) shows electrodes before and after prolonged use in a plasma source.

The greatest advances have been in ESI sources, which require, at minimum, a liquid analyte brought to a sharp tip using a channel of some sort, a contact and a counter electrode
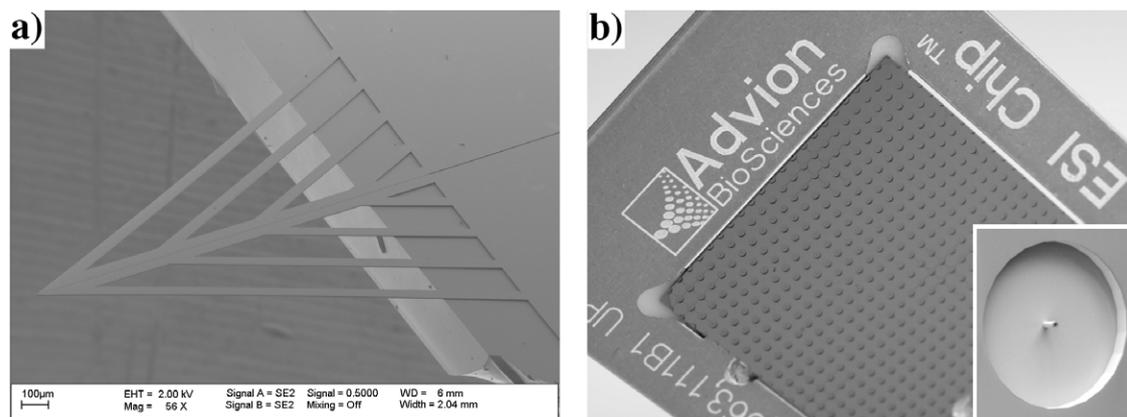
Figure 5. Microfabricated nanospray sources: (a) nib-type nanospray source (courtesy Professor Steve Arscott, Lille University); (b) Advion Triversa Nanomate® array-type source (courtesy Dr Jack Henion, Advion Inc.).
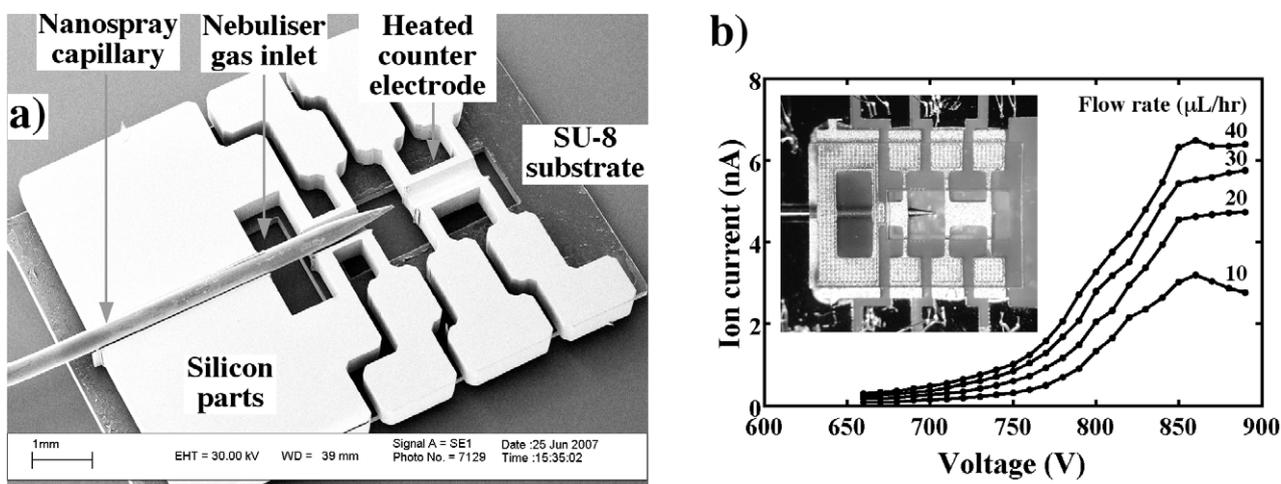

Figure 6. (a) Microfabricated electrospray ion gun (courtesy Microsaic Systems), and (b) emission characteristics [103] (courtesy Microsaic Systems; © 2007 IOP Publishing. Reproduced with permission. All rights reserved).

(often located on the mass spectrometer inlet) [87–91]. At the flow rates and channel dimensions used, the regime is universally nanospray, and chip-based sources have been constructed from glass [92], oxidized silicon and a wide variety of polymers [93], using capillaries, sealed channels, open channels and nibs [94, 95] for emission. For example, figure 5(a) shows a nib emitter formed as a cantilevered element in SOI [96]. More recent devices have been formed using nanopillar arrays [97] and even paper [98] as a wick. Sources with in-plane flow have been arranged as single elements and 1D arrays [99]. Geometries with through-wafer flow have been fabricated as 2D arrays [100, 101], and combined with sampling systems (for example, for rapid analysis of proteins separated by 2D gel electrophoresis [102]). Figure 5(b) shows the first commercial system, the Advion Triversa Nanomate®, which contains 400 nanoelectrospray nozzles formed by deep reactive ion etching.

Components designed to improve ionization efficiency, such as pneumatic nebulizers [103] and air amplifiers [104] have also been incorporated into chip based ESI sources. Figure 6(a) shows a V-groove mount for a conventional nanospray tip. Two such parts are used in a sandwich, as shown in the inset to figure 6(b). Each part is formed in etched Si

substrate on an SU-8 base, and the combination provides a complete ion gun that allows nebulization and heating of the spray. Emission begins at a threshold voltage of around 800 V (which is highly repeatable, due to the integration of a counter-electrode) and rises rapidly until a limit caused by spray instability [103]. Many other sources have also included upstream separation, and these will be described in section 6.4.

3.3. MEMS sample introduction methods

Until recently, the development of MEMS for sample introduction has received little attention. However, inlets with low gas conductance known as 'micro-leaks' have now been developed for planetary mass spectrometer probes, using serpentine channels etched in a silicon substrate, to achieve a low gas conductance within a small volume, together with an integrated inlet heater [105]. MEMS valves for similar applications have also been demonstrated [106].

Similarly, most nanospray sources have been designed for use with a conventional ESI-MS instrument, leaving miniaturization of the latter as an unsolved problem. A major advance has been the demonstration of a chip-based vacuum interface that allows ions generated at atmospheric pressure to be transferred
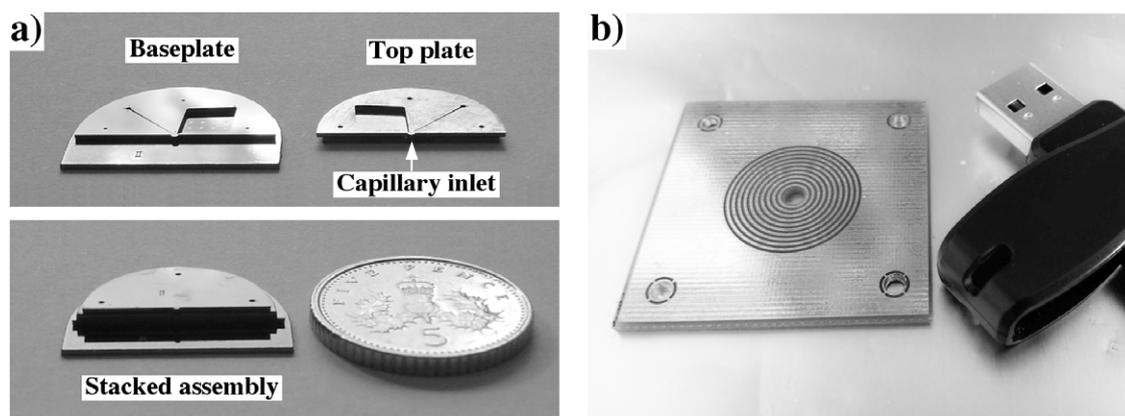
Figure 7. Microfabricated interface devices: (a) vacuum interface (courtesy Microsaic Systems); (b) planar ion funnel (courtesy Professor Tim Short, SRI International).

into vacuum for analysis [107]. The device is a multilayer silicon stack with deep etched capillaries for ion entrance and exit and a differentially pumped intermediate chamber. Figure 7(a) shows the components of an early device, before and after assembly into a two-part stack. Microfabricated components designed to increase the ion density in the entrained gas, such as ion funnels, have also been developed in microfabricated form [108, 109]. For example, figure 7(b) shows the concentric ring electrodes of a planar RF ion funnel. Further work is required on such components, since they represent the key to improving the sensitivity of small instruments.

4. MEMS mass filters

4.1. General background

Mass spectrometry is an old field, and approaches to mass filtering are described in several reviews [110–113]. Filtering involves the separation of ions based on their mass-to-charge ratio. For an ion of mass m and charge $q = ze$, where z is the charge number, the mass-to-charge ratio is m/z. Separation is carried out using electric and magnetic forces applied in vacuum. Assuming an ion velocity $\mathbf{v}$, an electric field $\mathbf{E}$ and a magnetic flux density $\mathbf{B}$, the force is $\mathbf{F} = q(\mathbf{E} + \mathbf{v} \times \mathbf{B})$. This force results in an acceleration a from Newton's law. Integration of the dynamical equation yields the trajectory. For example, for an electric field E in the x-direction, $qE = m\, \mathrm{d}^2x/\mathrm{d}t^2$. However, $E = \mathrm{d}V/\mathrm{d}x$, where $V(x)$ is the potential. Introducing the velocity $v = \mathrm{d}x/\mathrm{d}t$ we can write $\mathrm{d}^2x/\mathrm{d}t^2 = v\, \mathrm{d}v/\mathrm{d}x$. Consequently, $q\, \mathrm{d}V/\mathrm{d}x = mv\, \mathrm{d}v/\mathrm{d}x$. Integration from rest over a potential difference V_a then yields $qV_a = 1/2mv^2$, so the ion velocity is $v = \sqrt{(2qV_a/m)}$. However, for ions to follow this trajectory, collisions must be minimized. From kinetic theory, the mean free path λ in a gas with a molecular collision diameter d at pressure P is $\lambda = k_BT/(\sqrt{2\pi d^2 P})$. Typically, λ must be larger than the flight path, implying that low pressures are needed. One potential advantage of miniaturization is an increase in allowable pressure, with (for example) a ten-fold reduction in the ion flight path allowing a ten-fold increase in working pressure.

Any combination of fields that can induce different trajectories for different m/z can be used. However, separation is complicated by uncertainty in the initial position of the ion, coupled with its thermal velocity, which has a random direction and a root-mean-square value $v_{th} = \sqrt{(k_BT/m)}$. Significant additional refinements are required to overcome these effects, so ions with a given m/z are focused together. Key performance indicators are the sensitivity, mass range m_{max}, and mass resolution $m/\Delta m$ (where Δm is the mass spectral peak width), which defines the ability of the system to distinguish different ions. Below, we describe each of the mass filter types that have been miniaturized.

4.2. Magnetic sector instruments—background

The earliest MS systems were magnetic spectrographs [114], as shown in figure 1(a). These systems use a static flux applied perpendicular to the velocity vector to cause the ions to follow circular trajectories whose radius can be found from a balance between the magnetic and centrifugal forces qvB and mv^2/r, as $r = (m/q)\,(v/B)$. Assuming the velocity has resulted from a potential V_a as described earlier, $m/z = er^2B^2/2V_a$. Consequently, different m/z give different radii, and the dispersion can be observed on film or a detector array. The ion path can be partially straightened using an additional, perpendicular electric field, in the Wien filter [115], as shown in figure 1(b). Steady advances and major scientific achievements were made (the discovery of new elements) but large magnets were required, and early instruments were extremely bulky.

Unfortunately, miniaturization (which involves reducing r) requires a corresponding increase in B, and the achievable value is limited by magnetic saturation. In a given magnet design, volume and mass are inversely proportional to the energy product $\mathbf{B} \times \mathbf{H}$ of the magnet material. The most common compositions based on Al–Ni–Co–Fe (the Alnico series) have energy products of 5–6 MGOe. However, alternatives such as Nd–B–Fe allow the energy product to be raised to 45–50 MGOe. When combined with a high permeability yoke in V–Co–Fe (Hyperco 50A, saturation flux 22 000 G), a useful reduction in size could be obtained. Mattauch–Herzog
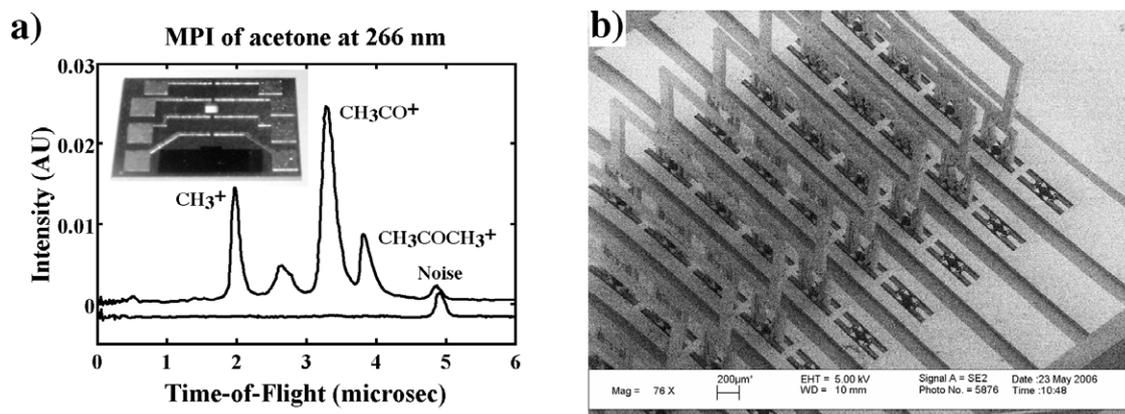
Figure 8. Microfabricated TOF-MS: (a) surface micromachined device, and spectrum of acetone (courtesy Professor Hyeun Joong Yoon, South Dakota State University, reprinted from Yoon H J *et al* 2002 *Sensors Actuators* A **97–8** 441–7, copyright 2002 [123] with permission from Elsevier); (b) plug-assembled reflectron electrode stack (courtesy Professor Guido Verbeck, University of North Texas).

double-focusing spectrographs (an electrostatic sector followed by a magnetic sector) have been demonstrated [13, 16], and spectrometers based on superimposed 90° electric and magnetic sectors (which can operate using a single detector) were developed using similar materials [17]. However, the fundamental problems of magnetic analysers were soon recognized.

4.3. MEMS magnetic sector instruments

Despite the above, attempts have been made to construct MEMS magnetic mass filters. For example, a Wien filter has been developed at Northrop Grumman, USA [116, 117]. The device is based on a continuous ion source, crossed magnetic and electric fields, and a detector array. The whole analyser except for the source is formed in a shallow cavity, measuring 1500 μm $\times$ 100 μm $\times$ 1 cm, etched into a silicon substrate, as shown in figure 2(b). The main advance was to provide a uniform in-plane transverse electric field using an electrode array, despite the presence of nearby grounded magnet poles. A mass range of $m/z = 40$–200 and a mass resolution $m/\Delta m$ of 150 were achieved, and a partially resolved spectrum of Xe isotopes (m/z 128–132) was recorded. A MEMS Wien filter has also been fabricated at CEA LETI (France) [118], using electrodes formed by DRIE of BSOI, with connections being made via etched grooves in the substrate. Two stacked wafers then formed a complete filter. Mass filtering was demonstrated, but with poor resolution. Proposals have also been made to fabricate MEMS magnetic sectors [119].

Recently, 1D and 2D coded apertures formed by DRIE of 250 μm thick silicon wafers have been used to increase the sensitivity of conventional sector instruments [120, 121]. The traditional object slit is replaced with a set of slits of varying size. Following dispersion of the component ions, a convoluted image of the coded aperture is recorded with an imaging detector, and deconvolution allows reconstruction of the spectrum. Throughput is dependent on the open area of the aperture while resolution is determined by the minimum feature size. An order of magnitude increase in sensitivity with no loss of resolution was achieved using a 1D aperture with a minimum feature size of 125 μm.

4.4. Time-of-flight analysers—background

An alternative approach that does not require a magnet is time-of-flight (TOF) filtering [122], previously shown in figure 1(d). A TOF mass spectrometer consists of a pulsed ion source, a drift tube of length L and a detector. An ion pulse entering the tube at $t = 0$ will exit at $t = L/v$. Assuming the velocity has resulted from a potential V_a, $m/z = 2eV_a\tau^2/L^2$. Consequently, ions with different m/z have different arrival times, and their presence can be distinguished as peaks in a detected signal. However, uncertainty in the initial position and velocity must be compensated to obtain sharp peaks. Space and velocity focusing were introduced in the first commercial instruments, and an improved method of compensation (the reflectron, a stack of reflecting electrodes) was then developed.

TOF mass spectrometers have an inherently high mass range. However, miniaturization (which involves a reduction in L) requires a reduction in ion velocity, which becomes increasingly difficult as the thermal velocity is approached. The necessary electrodes are planar and can be constructed from photoetched metal or PCBs. The key difficulty has been to obtain sufficient separation in a short distance, since the difference in arrival time Δt of ions with a difference in velocity Δv near a velocity v is $\Delta t = L(\Delta v/v^2)$, and v itself cannot be reduced arbitrarily because of thermal velocity effects. PI and MALDI have both been used to generate a short initial pulse of ions, and systems with Wiley–McLaren electrodes and reflectrons have been developed to compensate for uncertainty in initial ion position and velocity. The most successful work has been at Johns Hopkins University, who obtained impressive results with bench-top and portable systems (the 'Tiny-TOF' and 'Suitcase-TOF'). This group extended their work to TOF arrays, tandem TOF systems based on dual reflectrons and curved field reflectrons (which provide improved focusing) [18, 19].

4.5. MEMS time-of-flight analysers

Several chip-based TOF-MS systems have been demonstrated, using metal electroplating or deep silicon etching to form electrodes in the Wiley–McLaren geometry. In the earliest of these

[123], four pairs of shallow nickel electrodes were patterned onto an oxide covered silicon substrate (10 mm × 10 mm) to define electron extraction, sample ionization, ion acceleration, and ion drift regions. A suspended tungsten filament and a repeller electrode were also provided, as previously shown in figure 4(a). While thermionic emission from the filament was observed [66], ionization of the sample gas was not demonstrated. However, acetone fragments were detected when UV light from an external pulsed laser was focussed through a hole in the acceleration region (which obviated the need for on-chip pulsed ion injection), leading to the mass spectrum shown in figure 8(a). A considerably more sophisticated system incorporating orthogonal ion injection optics and a reflectron has been developed at CEA-DAM [68, 124] and used to record spectra of ethanol, argon, krypton, and xenon. The flight tube was created by DRIE of an upper silicon wafer and the reflectron was defined by patterning a resistive layer deposited on a lower glass wafer.

Discrete components for TOF-MS have been fabricated by The University of North Texas and Zyvex [125]. One of these, a Bradbury–Nielsen gate, is used to produce ion pulses. It consists of an array of parallel wires that prevent transmission when alternate wires are at different potentials and allow transmission when all wires are at the same potential. A grid of suspended silicon wires was fabricated using DRIE. Gating was demonstrated by placing the grid between an electron source and a detector. A reflectron comprising fifteen planar silicon electrodes plugged into a silicon motherboard was also manufactured, as shown in figure 8(b). Although a signal was detected following pulse extraction of ions, resolved peaks were not observed, due to the large pulse width and short path length.

The most advanced MEMS TOF mass spectrometer is the integrated system developed at TU Hamburg-Harburg [126]. Electrostatic gates are provided both before and after the drift region. The first gate chops the ion beam and the second gate allows transmission only of ions within a narrow time window. A mass spectrum is acquired by scanning the delay between the gating pulses. To increase resolution, ions are filtered with an electrostatic energy analyser between the drift region and the detector. The system is fabricated by DRIE of silicon-on-glass, using a single mask. The resolution is sufficient to resolve peaks corresponding to N^+, Ne^+, N_2^+, and Ar^+ at $m/z = 14$, 20, 28, and 40, respectively.

In general, many MEMS MS components are scaled versions of conventional designs, often with compromises imposed by the restrictions of planar processing. However, in some instances, unorthodox architectures can be realized. One example is a TOF instrument for space science applications in which initial ion pulses are produced by chopping the incoming flux with a micromechanical shutter fabricated on SOI [127]. The shutter operates at 306 kHz and has an open time of 100 ns.

4.6. Radio frequency filters, traps and ion guides—background

Two other methods that again do not require a magnet use time-varying inhomogeneous electric fields: the quadrupole filter show in figure 1(e) [128] and the quadrupole ion trap

shown in figure 1(f) [129]. In the filter, four parallel electrodes with hyperbolic sections are used to generate a 2D potential $\phi(x, y) = \phi_0(x^2 - y^2)/2r_0^2$. Here, r_0 is the radius of a circle touching the electrodes, whose potentials are $\phi = \pm \phi_0/2$. This field exerts forces in the x- and y-directions on an ion moving in the z-direction. For a singly charged ion, the equations of motion are $m\, d^2x/dt^2 = -e\phi_0 x/r_0^2$ and $m\, d^2y/dt^2 = +e\phi_0 y/r_0^2$. Normally the potential varies as $\phi_0(t) = U - V\cos[\omega(t - t_0)]$, where $\omega = 2\pi f$, f is a frequency in the RF range, t_0 is the starting time and U and V are constants. In this case, normalized trajectory equations of the form $d^2u/d\zeta^2 + \{a_u - 2q_u\cos[2(\zeta - \zeta_0)]\}u = 0$ are obtained. Here, $\zeta = \omega t/2$, $\zeta_0 = \omega t_0/2$, $a = 4eU/(m\omega^2 r_0^2)$ and $q = 2eV/(m\omega^2 r_0^2)$, u is x or y, $a = a_x = -a_y$ and $q = q_x = -q_y$.

Numerical integrations of the type previously shown in figure 3(a) show that the trajectory can be bounded or divergent. Its nature depends little on the initial conditions ζ_0, $u(0)$ and $u'(0)$, instead being determined almost entirely by a and q. Several regions on the q-a plane give stable solutions. The lower region is approximately triangular, and bounded by the loci $a_0(q) = q^2/2 - 7q^4/128 + 29q^6/2304$ …. and $b_1(q) = 1 - q - q^2/8 + q^3/64$ …. that define the limits for stability in the y- and x-directions, respectively. Between the two, trajectories are stable in both directions. The apex of this region is at $a = 0.237$, $q = 0.706$, so that $a/2q = U/V = 0.168$. In a quadrupole mass spectrometer (QMS), U and V are ramped together, following a line passing just below the apex. Stable trajectories are only obtained for a narrow mass range, so the device acts as a tuneable mass filter.

The mass resolution varies as $m/\Delta m \approx n^2/20$, where n is the number of RF cycles experienced by an ion. If the ions are injected with axial energy V_a, the number of cycles is $n \approx fL/v$, where L is the quadrupole length, so $\Delta m \approx 40eV_a/(f^2L^2)$. The maximum mass is limited by the potentials that can be applied. However, since U and V depend on r_0^2, decreasing the size by (say) 10 will reduce both potentials 100-fold. Conversely, Δm increases as L is reduced. Compensation can be provided through an increase in frequency, but this in turn requires an increase in voltage. QMS systems are workhorse instruments, with a good combination of range, resolution and sensitivity.

When the dc potential is omitted, the mass filtering action is largely lost. However, RF-only quadrupoles can guide ions in a 'pseudopotential' derived from the time variation of the inhomogeneous field. If ion guides are placed in an intermediate high-pressure cell containing a neutral background gas, energetic collisions can cool or fragment the ions. In the triple quadrupole (or QQQ), a first quadrupole filter is used for precursor ion selection, an RF-only quadrupole or ion guide is used for collision-induced dissociation, and a second quadrupole filter is used for analysis of the resulting fragments. This form of so-called 'tandem' mass spectrometry (MS-MS or MS^2) has much greater discriminatory power, since it allows differentiation of ions with the same m/z [130]. Alternative filters can be used for selection or analysis, leading to other tandem systems including Q-TOF and TOF-TOF. However, the need for multiple stages increases system complexity.
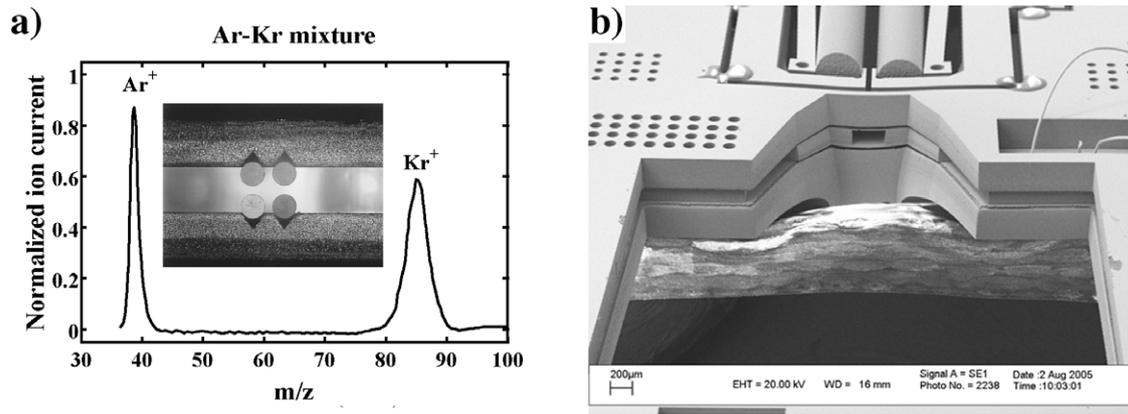
Figure 9. Microfabricated quadrupole filters: (a) V-groove type with spectrum of Ar–Kr mixture (data courtesy Professor Steve Taylor, Liverpool University); (b) BSOI type (courtesy Microsaic Systems).

An alternative approach is to confine ions in a trap, and release them in a mass selective operation. The quadrupole ion trap (QIT) is effectively a quadrupole filter wrapped round in a circle whose radius is then shrunk down to eliminate the inner electrode. Toroidal traps (in which the inner electrode is retained) have a larger trapping volume, and the linear ion trap (LIT), effectively a quadrupole filter with end-electrodes, has an even larger volume. A rather different type of trap, the Orbitrap [131], also exists, but has not so far been miniaturized. In contrast to continual filters, all ion traps have a duty cycle. However, they allow tandem mass spectrometry to be performed using a sequence of operations in a single component and hence enable very compact instruments.

The main difficulty encountered when miniaturizing RF mass filters and ion traps lies in realising the necessary 3D electric fields with sufficient accuracy, since any deviation can cause major perturbations to ion trajectories under the conditions used for selective filtering, which are normally manifested as a reduction in mass resolution. Two approaches have been used. The first is dimensional optimization of simpler surfaces such as planes and cylinders to approximate the fields generated by hyperbolic electrodes. The second is the use of planes carrying multiple electrodes, each held at a different potential.

Quadrupole filters, ion guides and linear ion traps (LITs) have all been miniaturized using cylindrical rods with optimized radii and separation in place of hyperbolic electrodes. Using conventional technologies, NASA and its contractors developed array-type quadrupoles to recover the sensitivity lost by miniaturization [20–22]. Because it can be constructed as a three-layer stack, with each layer simply containing a hole, the cylindrical ion trap (CIT) has proved extremely popular. The CIT uses optimized electrode radii and separations to approximate the 3D electrostatic fields normally generated in a QIT using precisely machined hyperbolic surfaces. However, the most impressive work has been that of Cooks at Purdue University, who has developed many miniature filters, including CITs, LITs and trap arrays [23–26]. Many variants have subsequently been demonstrated (for example, LITs with hyperbolic electrodes formed by rapid prototyping [27, 28]).

Segmented electrodes, which involve a set of planar electrodes held at different potentials, allow 3D fields to be realized without the need for shaped electrodes, and have been extensively investigated at Brigham Young University. Examples include segmented-electrode cylindrical and linear ion traps [132, 133], and the 'halo' ion trap [134, 135], which approximates a toroidal trap. Brigham Young have also developed continuous resistive electrodes, which again allow 3D fields to be generated, but from a single potential.

4.7. MEMS RF filters, traps, and ion guides

Early attempts to fabricate MEMS quadrupole filters with an out-of-plane ion path were made by JPL [136], using a synchrotron to expose a 1 mm layer of thick photoresist and replicating the resulting mould in electroplated nickel. However, the very short ion path and small pupil presented intrinsic performance limitations. Much greater success has been achieved by mounting cylindrical metal electrodes with diameters of around 0.5 mm and lengths of a few cm into microfabricated silicon mounts, and filters with out-of-plane rods have been constructed using deep-etched silicon mountings at MIT [137].

Filters with in-plane rods have been constructed as shown in figure 2(a) using a pair of stacked, oxidized Si wafers carrying V-groove alignment features for 30 mm long metal-coated glass electrodes and glass spacer rods [138–141], in a joint project between Imperial College and Liverpool University. Here the challenge was to minimize the effect of the grounded substrate on the electric field. Figure 9(a) shows a completed device, together with an early spectrum (for an Ar–Kr mixture). Although the peaks are distinct, the resolution is clearly insufficient to separate adjacent elements. In addition, the mass range was limited to $m/z \approx 100$ by the thin oxide insulator, which resulted in RF heating, differential thermal expansion and eventual rod detachment. Although additional components such as 1D coupling lenses were also demonstrated [142], the range of features that could be provided by bulk micromachining was a fundamental limitation. However, such early results provided evidence that chip-based MS was possible.
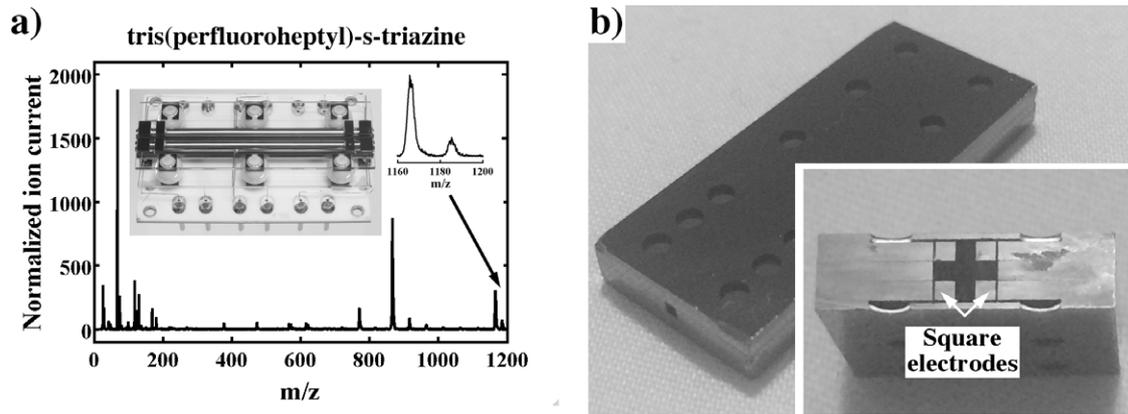
Figure 10. Microfabricated quadrupole filters: (a) silicon-on-glass type, and mass spectrum of tris(perfluoroheptyl)-s-triazine (courtesy Microsaic Systems, © 2010 IEEE, reprinted with permission, from Wright S *et al* 2010 *J. Microelectromech. Syst.* **19** 325–37 [144]); (b) BSOI type with square electrodes (courtesy Professor Luis Velásquez-García, Massachusetts Institute of Technology).
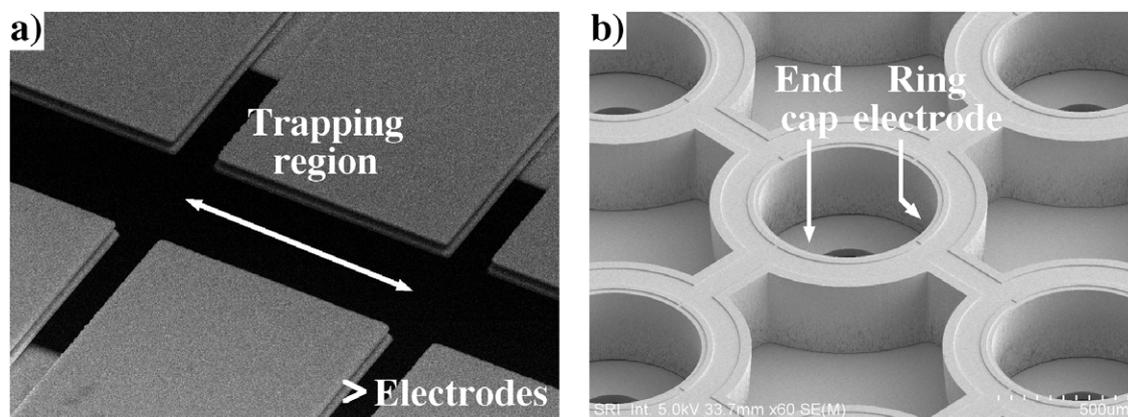

Figure 11. Microfabricated ion traps: (a) linear trap in GaAs (courtesy Dr Chris Monroe, University of Maryland, adapted by permission from Macmillan Publishers: *Nature Phys.* [148], © 2006); (b) cylindrical trap in BSOI (courtesy Dr Tim Short, SRI International).

A more advanced system was developed by the Imperial College spin-out company Microsaic Systems using BSOI [143], which allows improved oxide isolation, removal of the surrounding silicon, and fabrication of sliding spring mounts for metal rods and additional ion coupling optics as previously shown in figure 3(b). Figure 9(b) shows the completed device, near the exit pupil, showing the spring mounted rods and output coupling optics. As a result, the mass range could be increased to $m/z \approx 400$ and such filters formed the basis of the first commercial MEMS mass spectrometers.

A further iteration has used anodically bonded silicon-on-glass substrates, separated using balls in sockets rather than rods [144]. The glass provides isolation comparable with conventional quadrupoles, and has allowed the mass range to be increased to $m/z \approx 1200$. Figure 10(a) shows the filter on a sub-mount, together with a spectrum of tris(perfluoroheptyl)-s-triazine that highlights the performance improvements made since the demonstration of early V-groove devices. Microsaic has also demonstrated RF-only (or Brubaker) pre-filters (which increase ion coupling), RF-only ion guides (which improve ion transfer in intermediate pressure stages) and collision cells.

Recently, there has been interest in using square electrodes to generate approximations to hyperbolic fields. This approach

allows the electrodes to be batch fabricated using DRIE, drastically reducing fabrication cost [145, 146]. Figure 10(b) shows the device, together with a cross-section sawn to expose the electrodes. The filter operates in a higher region of the stability diagram, and useful performance has already been obtained. Quadrupole filters and a wide variety of linear ion traps have been proposed using similar approaches [147]. For example, figure 11(a) shows a LIT formed as a multilayer stack in GaAs-based technology, with the gaps between electrode sections defining the trapping region [148].

Many quadrupole ion traps have been fabricated by using different processes to form the holes needed in the cylindrical electrode approximation. In each case, CITs have been formed as single elements and as arrays, with a trapping volume limited by the substrate thickness. The simplest methods yield single layers, which must be arranged into the CIT geometry by stacking, using insulating interlayers. Suitable processes include plug assembly [125], drilling (for metals) [149, 150], punching and metal-coating (for low temperature co-fired ceramics) [151] and deep etching (for silicon) [152–154]. Figure 11(b) shows a deep-etched component for a CIT formed as previously described in figure 2(c), showing the central ring electrode and one of the end-caps. Two such dies, placed back-to-back, form a complete trap. In this case,
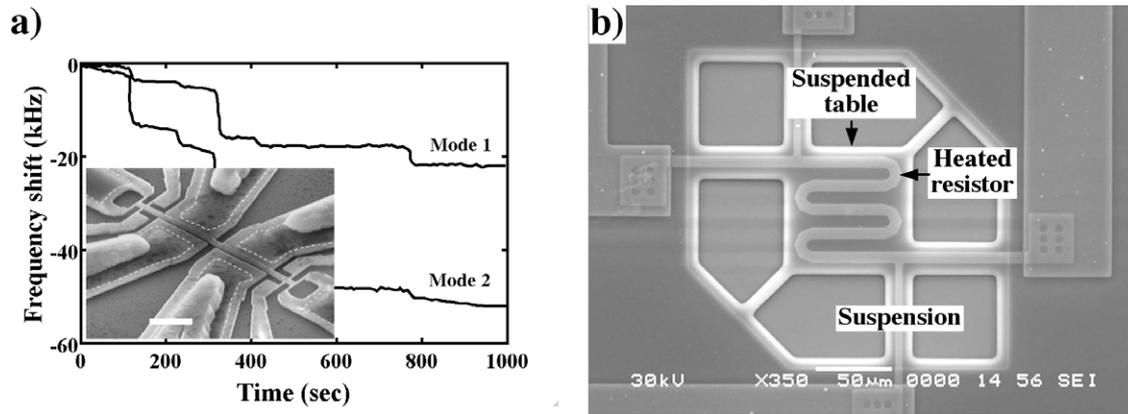
Figure 12. MEMS sensor components: (a) mechanical mass detector and its time response (courtesy Professor Selim Hanay, California Institute of Technology, adapted by permission from Macmillan Publishers: *Nature Nanotechnol.* [171], © 2012); (b) thermal conductivity vacuum gauge (courtesy Professor Zhenan Tang, Dalian University of Technology).

construction of an array is made simpler and can be used to compensate for the loss in sensitivity caused by size reduction.

Integrated approaches, which involve patterning and etching multiple layers of deposited material, yield three-layer electrode stacks directly. In this case, the volume is limited by the thickness of material that can be deposited. The most complex design used a multilayer 'Damascene' process developed at Sandia National Laboratory [155]. SiO_2 is first deposited on an insulated Si substrate, and patterned and etched to form a mould. The mould is then filled with tungsten by chemical vapor deposition, and the surface is planarized using chemical–mechanical polishing. This cycle is repeated seven times to form all three electrodes and spacers, with a final layer containing connections and an ion collector. Finally, the SiO_2 is removed to leave a free-standing tungsten structure.

5. MEMS ion detectors, vacuum gauges and pumps

5.1. Ion detectors—background

The simplest electronic ion detector is the Faraday detector, which uses a metal electrode to collect incident ions and an amplifier to produce a measurable current. Faraday detectors offer good stability and linearity, but sensitivity is limited by intrinsic thermal and shot noise. To improve performance, secondary electron multipliers are almost universally used. Discrete dynode multipliers comprise a staggered set of electrodes in a material with a high secondary electron yield, such as Be–Cu alloy. A resistor network establishes a potential difference between each of the 10–20 electrodes. Ions impinge on the first electrode (the conversion dynode), resulting in secondary electron emission. The electrons are accelerated towards the next electrode where they induce further emission. If the secondary yield is greater than unity, there is amplification at each stage and a total gain of $>10^6$ is common. The avalanche is collected and measured as integrated charge or a discrete pulse.

Continuous dynode (or channel) multipliers were proposed by Farnsworth in 1930 and developed in the 1960s. Channel multipliers are lead silicate glass tubes with curved internal channels. Treatments applied to the glass leave a thin surface layer with secondary electron emissive properties and a buried semiconducting layer that can be used to establish a potential gradient without an external resistor chain. Ion impacts initiate electron emission. The secondary electrons are accelerated by the applied potential and collide with the sidewall, generating further secondary electrons. Multiple impacts then result in a measurable integrated charge at the collector. Microchannel plates (MCPs), which were originally developed for military night vision, use a similar principle. A typical plate comprises an array of 10^6–10^7 straight channels formed in a 1–2 mm thick lead glass substrate, with each channel measuring 10–15 μm in diameter. The gain of a single plate is approximately 10^4 but plates may be stacked for higher gain.

5.2. MEMS ion detectors

Because of the ease with which electrodes and electronics can be combined in silicon, integrated detectors have been demonstrated using arrays of Faraday cups [156–158] or charge-coupled devices (CCDs) [159]. However, there has been limited progress on multiplying detectors, due to the complex nature of the materials required (which must have a high secondary electron yield, and in continuous channel must also be semiconducting). MCPs have been made by deep etching silicon substrates [160, 161] and their emission properties have been improved with CVD diamond [162]. MCPs have also been combined with microelectronics for readout [163–165]. A small number of discrete dynode electron multipliers have also been demonstrated [166, 167]. However, the vast majority of MS systems still use channel electron multipliers.

An interesting new development is the use of resonant MEMS cantilevers [168, 169], beams [170, 171] and membranes [172–174]; these allow direct detection of the ion mass rather than its charge. Attachment of ions causes changes in resonant frequency proportional to the ion mass. Not only the mass but also the position of individual ions can be tracked by monitoring two different vibrational modes [171]. For example, figure 12(a) shows a vibrating beam resonator and the time variation of the frequency of two modes, showing

abrupt, correlated steps that correspond to ion attachment. Mechanical oscillations can also be detected via field emission of electrons from a membrane, allowing the detector to convert thermal energy deposited by ion bombardment into an electrical signal [173, 174].

5.3. Vacuum gauges—background

Gas pressure can be determined directly by using the force resulting from molecular impacts to deflect a moveable mechanical element or displace a liquid. Alternatively, it may be measured indirectly by exploiting a pressure-dependent property such as viscosity, thermal conductivity, or ion yield under ionizing conditions. Direct gauges measure true pressure whereas indirect gauge measurements depend on gas composition.

Direct pressure gauges based on the deflection of a membrane separating a reference pressure from an unknown pressure are widely used. For vacuum measurements the reference pressure is usually well below the working range of the gauge. The deflection of the membrane can be detected using a strain gauge, or by monitoring the change in capacitance between the diaphragm and a fixed electrode. In thermal conductivity gauges, heat loss from a hot wire due to the thermal conductivity of the surrounding gas is measured. As the pressure is reduced, radiation and heat conduction through the supports eventually limit the measurable pressure. In Pirani gauges, the hot wire forms one side of a Wheatstone bridge. Thermocouple gauges directly measure the temperature using a thermocouple junction attached to the wire.

5.4. MEMS vacuum gauges

MEMS pressure gauges that use the deflection of a diaphragm to measure a pressure differential are well-established [175]. However, these cannot measure low pressures accurately if the comparison pressure is atmospheric, and attempts to use evacuated cavities to provide a low-pressure comparison have only been marginally successful [176, 177]. The friction gauge, which uses damping of a resonator by residual gas as an indicator of pressure, has also had limited acceptance [178, 179]. The most common MEMS vacuum gauges are thermopiles and Pirani gauges. Both exploit cooling by residual gas. Thermopiles use the Seebeck effect in resistively heated silicon to generate a voltage, which is then reduced by any cooling [180, 181]. Pirani gauges are based on a heated wire formed in a material such as Pt with a high temperature coefficient of resistance. Suspension of the heated element on a slender support minimizes cooling by parasitic solid conduction, allowing much lower pressures to be sensed [182–184]. Figure 12(b) shows a modern MEMS thermal conductivity gauge with a meander resistor suspended on a small table. On-chip circuitry for heating, sensing and analogue-to-digital conversion can be incorporated [185–187]. MEMS thermal conductivity gauges are available commercially (e.g. 925™ Micropirani, from MKS Instruments [188]).

5.5. Vacuum pumps—background

Many types of vacuum pumps exist [189]. However, their mechanism can generally be characterized as positive displacement, momentum transfer, capture, or thermal. In positive displacement pumps, a rotating or reciprocating motion causes gas to be drawn in at the inlet, compressed, and expelled through the exhaust. Examples include vane, scroll, piston, roots, diaphragm, claw and screw pumps. In some cases, oil provides a seal between moving parts, while in others back-leakage is reduced by using high-accuracy machining to minimize clearances.

In momentum transfer pumps, gas molecules gain momentum through interaction with a supersonic vapour jet (diffusion) or a fast moving rotor (turbo). Diffusion and turbo pumps cannot pump down from atmospheric pressure or exhaust to atmosphere, as they work in the molecular flow regime. Consequently, a displacement pump must be used for evacuation and backing. The main challenge in miniaturizing a turbo pump is that the rotor speed must rise, so that the blade velocity (which must be a significant fraction of the average molecular velocity) is sufficient to pump lighter gases. For example the Creare Minivac turbo pump has a rotor diameter of 2.5 cm and achieves a pumping speed of $4\,\mathrm{l\,s^{-1}}$ with a rotor speed of 200 000 rpm [190, 191].

In capture pumps, gas molecules are condensed on cryogenically cooled surfaces, adsorbed by chemically active surfaces (gettering), or buried. Gettering involves chemisorption of gases by a reactive surface, often generated by sputtering of titanium. The surfaces of non-evaporable getter (NEG) pumps must be activated, by heating to 400 °C (which causes surface reaction products to diffuse into the bulk). In sputter-ion pumps, gas molecules are ionized by a Penning discharge between two Ti cathodes and a cylindrical anode, whose axis is aligned with a strong magnetic field. When the ions are accelerated in the electric field and impact a cathode they become implanted, but also sputter titanium, which deposits on the anode and opposing cathode. Hence, in addition to ion pumping, gas is removed by gettering at the fresh Ti surface. Thermal pumps exploit the temperature dependence of gas properties. In Knudsen pumps, a hot chamber is connected to a cold chamber by a narrow channel where molecular flow conditions exist. A net flow from the cold to the hot chamber is then established, as the rate of effusion from either side is proportional to $1/\sqrt{T}$.

Pumps are characterized in terms of their pumping speed, compression ratio, and ultimate pressure. The speed is $S = Q/P$, where Q is the throughput and P is the pressure at the inlet. In general, S is a function of P, and may also depend on the molecular mass of the gas. The compression ratio is the ratio of inlet pressure to outlet pressure. For diaphragm pumps, compression ratios of $10–10^2$ are typical, whereas for high vacuum pumps, values as large as $10^6–10^8$ are achieved. A pressure of $10–10^{-3}$ Torr can typically be achieved with positive displacement pumps, but lower pressures require momentum transfer or capture pumps.
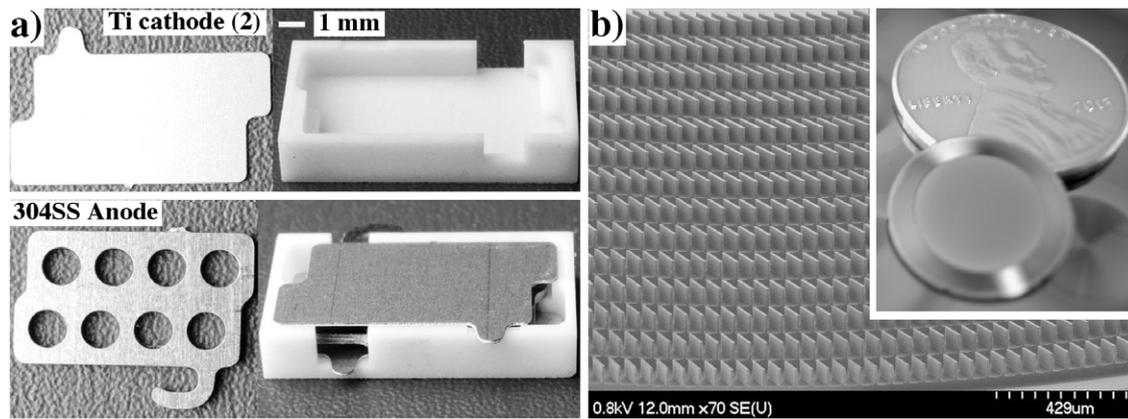
Figure 13. Microfabricated vacuum pumps: (a) components for a Ti sputter ion pump (courtesy Professor Yogesh Gianchandani, University of Michigan, © 2013 IEEE, reprinted with permission, from Green S R *et al* 2013 *J. Microelectromech. Syst.* **22** 309–17 [198]); (b) deep etched silicon turbo pump rotor blade (courtesy Dr Wei Yang, Honeywell).

5.6. MEMS vacuum pumps

Vacuum encapsulation technologies for MEMS devices such as gyroscopes, accelerometers, and RF switches are well advanced. Getter films are often deposited at manufacture to pump the small gas load due to outgassing and micro-leaks. Early attempts at fabricating micromachined pumps met with limited success, mainly because of the performance limits set by the poor dimensional scaling of dead volumes and clearances [192], and for some time the best-known example was the LIGA fabricated scroll pump developed at JPL [136]. However, there has recently been considerable progress, with significant developments arising from a DARPA program (Chip-Scale Vacuum MicroPumps) involving the University of Michigan, MIT, and Honeywell. It is now possible to envisage MEMS mass spectrometers with microfabricated pumps, although considerable development will be needed to achieve sufficient base pressure, pumping speed, and mechanical reliability.

Coarse vacuum can be generated relatively simply on-chip by gas–liquid phase transition [193]. Knudsen pumps are also well suited to chip-scale pumping and a number of attempts have been reported [194, 195]. There are no moving parts and the principal requirement is a series of chambers connected by channels. Performance can be improved using multiple pump stages. The most successful example is a 162-stage pump fabricated using a five-mask, single-wafer process [196]. With the pump inlet sealed, the pressure at the final stage decreased from atmospheric pressure to 0.9 Torr (a compression ratio of 844) after 30 h. Continuous operation was sustained for 37 d.

A micro-scale sputter-ion pump employing thin film titanium electrodes has been developed for vacuum-encapsulated MEMS [197]. Cells comprising of an inner circular anode and an outer concentric cathode were patterned in a titanium layer deposited on a glass substrate. An external magnet was not required as the plasma is spatially confined when the gap between electrodes is very small, and stable discharges can be maintained at pressures as high as 760 Torr. Miniature sputter ion pumps based on Penning cells have also been demonstrated [198], and orbitron pumps have been proposed [199]. Figure 13(a) shows the stainless-steel anode,

titanium cathode and overall assembly of a Penning-type sputter ion pump, which achieved a pressure of <10 mTorr after 4 h pumping.

As part of a broader effort to develop fully integrated mass spectrometers, a vapour jet pump has been developed at TU Hamburg-Harburg [200, 201]. The micromachined silicon pump incorporates a Laval nozzle to generate a supersonic jet of a working fluid. The gas throughput of more than 23 ml min^{-1} is impressive but the ultimate pressure was only 495 Torr after pumping from atmospheric pressure.

A pneumatically actuated four-layer silicon diaphragm pump capable of pumping from atmospheric pressure to 164 Torr has been fabricated using DRIE and wafer bonding [202]. The moveable components were defined in BSOI by etching through the handle layer to the oxide. The remaining 10 μm thick device layer is flexible and acts as the diaphragm, allowing actuation of the valves and piston. A high compression ratio was achieved, by minimizing dead volume. A similar electromagnetically actuated pump has also been demonstrated with a latex membrane [203].

A number of authors have discussed liquid [204] or vacuum [205] turbo pumps based on rotors fabricated by DRIE of silicon. Impressive results have been obtained at Honeywell, who have demonstrated a deep etched, electrostatically levitated rotor designed for radial pumping [206]. Figure 13(b) shows the blade array, together with a complete rotor on a spindle for testing. Vacuum is developed at the center of the rotor, with each ring of blades acting as a separate pumping stage. The pump is a hybrid device as other parts, including the casing, motor, and bearings, are small but otherwise conventional.

6. MEMS mass spectrometer systems

6.1. Modular systems

Complete MEMS MS systems can be constructed by combining individual components as modules, or by chip-level integration. However, the components often have widely varying pressure, temperature, electrical, and mechanical requirements. Arguably, the best route is to develop
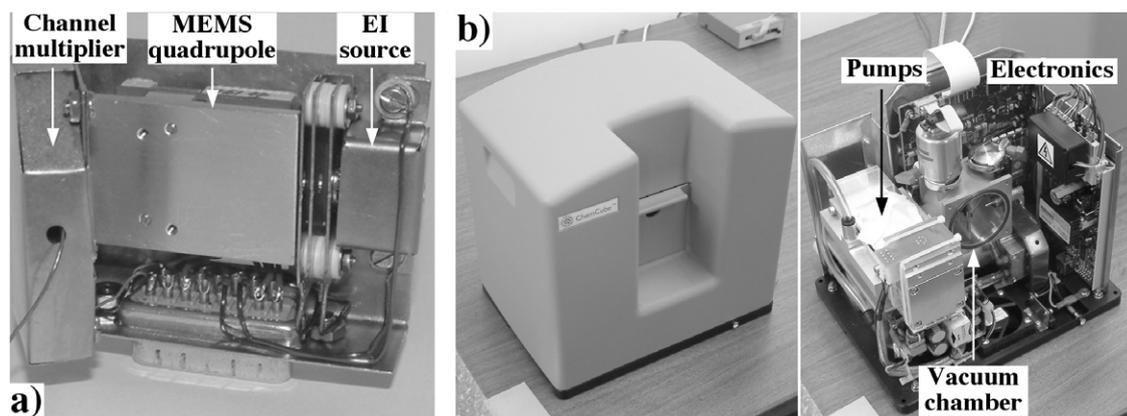
Figure 14. MEMS-based mass spectrometer sub-systems and systems: (a) IONCHIP quadrupole filter module; (b) Chemcube™ benchtop instruments, closed, and revealing chassis (all courtesy Microsaic Systems).
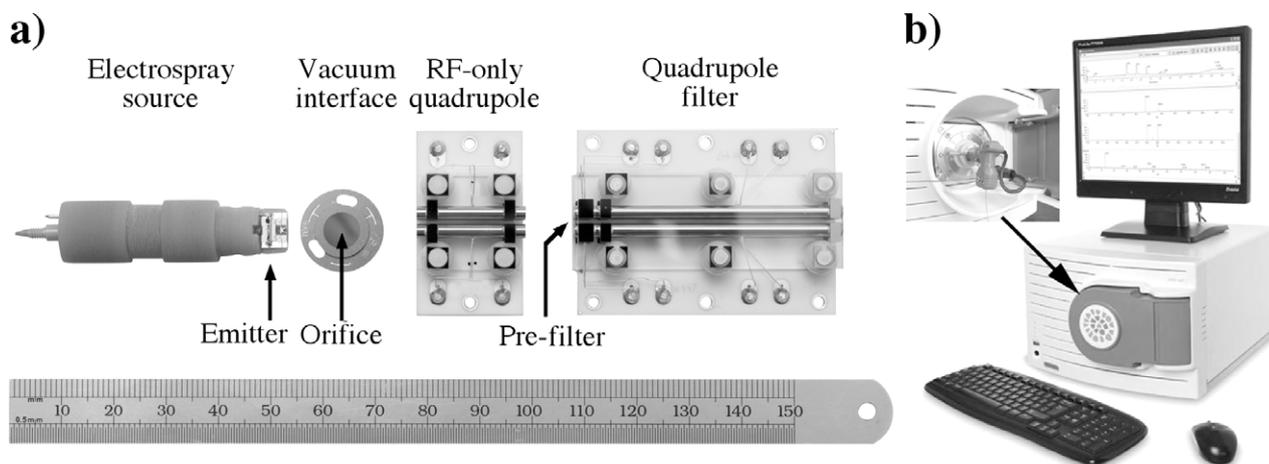

Figure 15. MEMS ESI-MS: (a) packaged sub-components, reproduced with permission from Malcolm A *et al* 2011 *Rapid Comm. Mass Spectrom.* **25** 3281–8 [11] (copyright © 2011 John Wiley & Sons, Ltd.); (b) Microsaic 4000 MiD (all courtesy Microsaic Systems).

sub-systems as separate modules, using MEMS or conventional techniques where appropriate. This has been the approach taken by Microsaic Systems.

In 2005, Microsaic developed a miniature benchtop system (ChemCube™) [207]. The core is a module comprising a MEMS quadrupole filter (IONCHIP, previously shown in figure 9(b)), a small conventional EI source, and a channel electron multiplier. Figure 14(a) shows the module, which has the filter at the centre, the source on the right and the multiplier on the left, each in a shielded enclosure. This module plugs into a connector in the base of a 220 cm^3 vacuum chamber, which is pumped by a 10 l s^{-1} turbo pump and a diaphragm pump contained in a compact chassis. Figure 14(b) shows the instrument with and without its enclosure. The pumping system is on the left and the chamber at the centre. To introduce an analyte, a SPME fibre is first exposed to the headspace above a sample and then pushed through a heated septum, where the analyte desorbs.

Other things being equal, the sensitivity of ESI-MS systems is dominated by the capacity of the pumping system. Miniaturization can therefore have a drastic effect. Despite this Microsaic has successfully developed MEMS ESI-MS instruments, the 3500 MiD [11] and later the 4000 MiD. Each

incorporates a nanospray source, a vacuum interface, an ion guide, and a high-performance quadrupole with a pre-filter, all packaged as MEMS modules as shown in figure 15(a). Figure 15(b) shows the 4000 MiD. No other components are required; the computer and pump system are both contained in the enclosure. The portal on the right-hand side allows access to the spray source, which receives the analyte via capillary tubing. Both instruments can be coupled to an HPLC system to form a complete LC-MS. A later variant has been incorporated into a flash chromatography system (Biotage Isolera Dalton [208]) and used to identify separated reaction products.

The use of PCBs as structural elements has been a key feature of modular systems. MEMS quadrupole filters and ion guides are conveniently supplied as header boards that plug into mating connectors on a base PCB. The pins and sockets provide electrical connections and structural support. Recently, a triple quadrupole mass spectrometer with six separate MEMS modules (ESI source, vacuum interface, ion guide, filter for precursor ion selection, collision cell for ion fragmentation, and filter for analysis of the resulting fragments) was demonstrated. The quadrupole components are each mounted on separate header boards that plug into a series
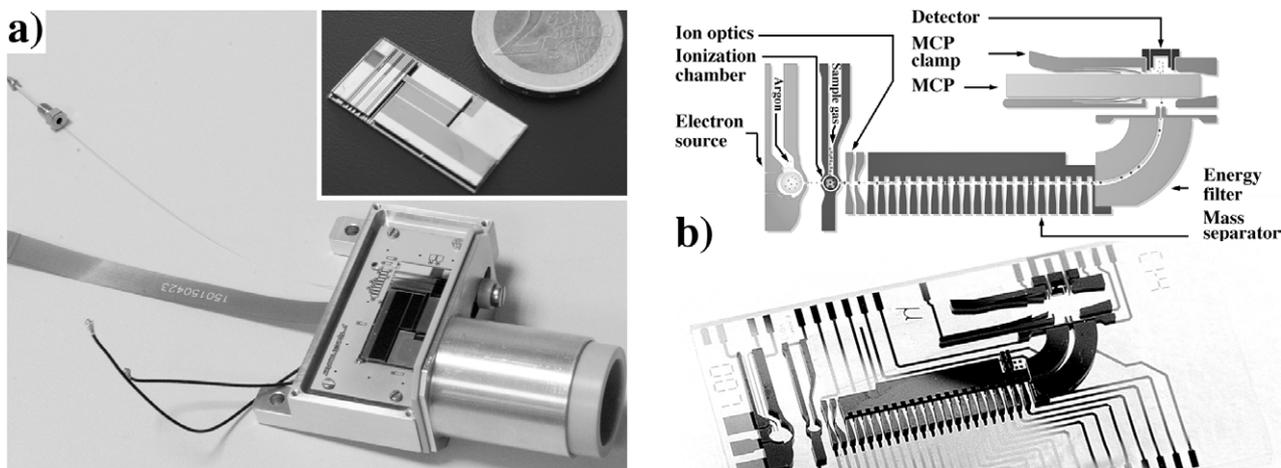
Figure 16. Integrated MEMS MS: (a) TOF-MS (courtesy Dr Charles-Marie Tassetti, CEA-DAM); (b) planar integrated micro mass spectrometer (courtesy Dr Grigory Quiring, TU Hamburg-Harburg).

of PCBs supported in a skeleton aluminium frame, revealing the power of MEMS to simplify complex instruments [209].

6.2. Mass spectrometer-on-a-chip

Several attempts have been made to increase chip-level integration, by combining a mass filter with a source or detector. Efforts have also been made to create an entire system in a microfabricated vacuum chamber. However, performance has generally been lower than for modular MEMS MS, partly due to the inherently lower sensitivity of smaller systems and partly to the fact that integration makes the optimization of individual components more difficult. Progress has also been slower, due to the higher costs of larger MEMS dies and the increased cycle times and lower yields associated with more complex dies.

Notable efforts on magnetic systems include the previously mentioned Wien filter developed by Northrop Grumman [116, 117], while non-magnetic systems include the TOF systems developed at CEA LETI/DAM [68, 124] and TU Hamburg-Harburg [126]. Figure 16(a) shows the CEA TOF-MS, which has an external filament, a chip-based analyser and an external MCP detector. The inset shows the analyser, which contains a grid for introducing electrons, an ionization chamber, an einzel lens for extracting and focusing ions, and a drift zone and a reflectron for mass analysis. The most complete system is the planar integrated micro mass spectrometer (PIMMS), also developed at TU Hamburg-Harburg and shown in figure 16(b). The chip integrates a microwave plasma ion source, ionization chamber, electron and ion extraction, acceleration and focusing, a novel mass filter (the synchronous ion shield, SIS), an energy filter and alignment features for a MCP detector, truly a tour de force [210–212].

6.3. Hyphenated systems—background

Complex mixtures are often separated into components before each is analysed in a mass spectrometer. Separation methods for gases include gas chromatography (GC) [213] and ion mobility spectrometry (IMS) [214] and its field-asymmetric variant

(FAIMS). Techniques for liquids include liquid chromatography (LC) [215] and capillary electrophoresis (CE) [216]. In LC and GC, separation occurs as the mixture is swept by the mobile phase through a column containing a stationary phase. IMS and CE separate ionic components according to their drift velocities in an electric field. Systems that follow separation with analysis are described as 'hyphenated'. The first such technique was gas chromatography-mass spectrometry (GC-MS). Later techniques include liquid chromatography-mass spectrometry (LC-MS), capillary electrophoresis-mass spectrometry (CE-MS) and ion mobility spectrometry-mass spectrometry (IMS-MS).

6.4. MEMS hyphenated techniques

Following the demonstration of a silicon gas chromatograph [217], MEMS GCs have been extensively developed. Columns have been fabricated in parylene [218], silicon oxynitride [219] and nickel [220], and packed with a range of stationary phases including plasma polymerized poly(dimethylsiloxane) (PDMS) [221], functionalized parylene [222], monolayer-protected gold [223], and atomic-layer deposited alumina [224]. Figure 17(a) shows a modern semi-packed column, formed using etched and coated pillar arrays to avoid difficulties with particulate filling. Columns have been formed in arrays [225], and integrated with sample injectors [226], temperature controlled heaters [227], pumps and preconcentrators [228] and photoionization detectors [229]. Portable GC units have been constructed [230, 231], and portable GC-MS systems have been demonstrated using valved injectors and electron ionization [232, 233]. However, the development of MEMS GC has taken place entirely separately from that of MEMS MS.

Similar developments have occurred in ion mobility spectrometry; although microfabricated IMS and FAIMS devices have been demonstrated [234–239], these have been developed as separate units, and no combined MEMS IMS-MS system has appeared. However, MEMS-based FAIMS instruments such as the Owlstone Lonestar Gas Analyser [240] have been available commercially for some years.
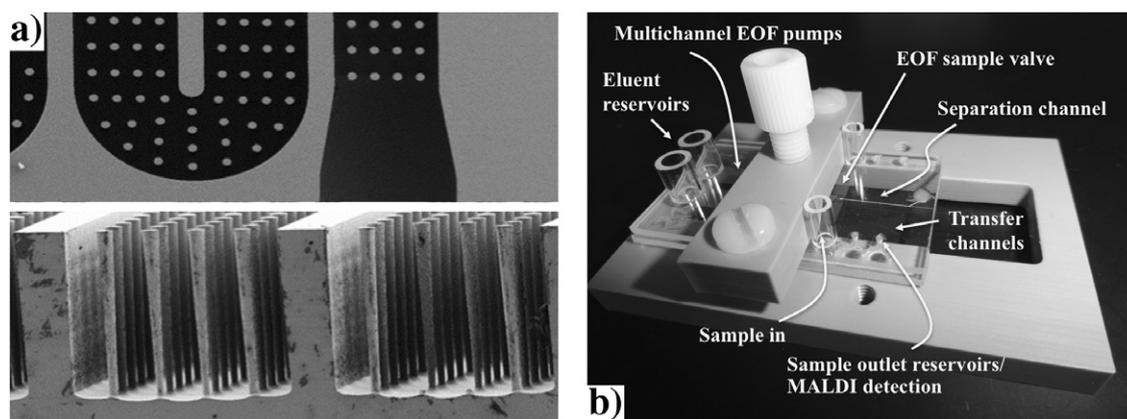
Figure 17. Microfabricated separation systems: (a) semi-packed GC column (courtesy Professor Masoud Agah, Virginia Tech, reprinted from Shakeel H *et al* 2014 *Sensors Actuators* B **203** 641–6 [224], copyright 2014 with permission from Elsevier); (b) LC column with orthogonal sample extraction for MALDI-MS [252] (courtesy Professor Iuliana Lazar, Virginia Tech).

In contrast, the coupling of chip-scale LC and CE to MS is an area of considerable activity, and the field has been extensively reviewed [45, 46, 87–91, 241–243]. In each case, the advantage is that small samples can be processed without excessive dilution, resulting in high detection sensitivities. As the analytes are in solution, ionization is almost exclusively by nano-ESI [57, 58]. In many cases, the separator and nanospray source are distinct components; in others they are monolithically integrated. The latter approach is more challenging but the lower dead volume reduces peak broadening and chromatographic delay.

Development of MEMS LC has followed a similar course to MEMS GC. Following original demonstration in Si [244], chip based high performance liquid chromatography (HPLC) systems were developed to operate at higher pressures [245, 246]. Flow is typically generated using external pumps, although electrolytically generated gas has also been used to displace liquid from reservoirs [247, 248]. Columns have again been fabricated in other substrates, including glass [248] and PDMS [249], and packed with particulates [250] and pillar arrays fabricated by DRIE [251]. Figure 17(b) shows an LC column designed for use with matrix-assisted laser desorption ionization [252]. The chip combines eluent reservoirs, sample reservoirs, valves, channels for pumping by electro-osmotic force, separation channels and outlets for MALDI to allow subsequent analysis.

Co-integration with nanoelectrospray tips soon followed. For example, Agilent have developed a chip LC mounted between the rotor and stator of a mechanical valve, allowing sample introduction and coupling to an LC pump [253, 254]. The is constructed from laminated polyimide films with laser ablated channels, and a conical, micromachined nanospray tip. Another system [247] combines a packed column, a low volume mixer and an electrospray nozzle, and is fabricated by lithographic patterning of parylene on a silicon substrate. Stationary phases have also been fabricated as porous monoliths by polymerization of a liquid precursor [255, 256], or as deep-etched silicon micropillar arrays that are subsequently coated with a polymer stationary phase [257, 258].

Chip-based CE systems are simple, requiring only a separation channel with appropriate electrodes. However, because of the voltages involved, substrates are insulating. The original demonstrations used glass [259], but injection-molded plastics [260], poly methyl methacrylate (PMMA) [261] and PDMS [262] are all common. CE was again rapidly integrated with nano-ESI. A wide variety of substrates and processing techniques have again been used, including photolithography and wet etching of glass [263], laser micromachining of polycarbonate [264], casting of PDMS [265], lithographic patterning of SU-8 resist [266, 267], and UV embossing of the inorganic–organic hybrid Ormocomp [268]. Internal polymer monoliths may also be incorporated, using *in situ* casting [269]. A complication is that the buffers needed for electrophoresis are not well suited to electrospray. Consequently, the analyte is often mixed with another solvent at the emitter tip, in so-called sheath flow. Chip-based CE-ESI is widely used with conventional mass spectrometers; however, miniaturized CE-MS systems are starting to be developed [270].

7. Applications

7.1. Portable systems

Many universities, companies and government laboratories have constructed battery-powered portable MS systems based on conventional technology, typically using an EI source and a miniaturized filter. Cylindrical [271] and linear [272, 273] ion traps have been developed at Purdue University and its spin-out Griffin (renamed ICx Technologies and now part of FLIR Systems (current product: Griffin 460, linear ion trap [274]). 908 Devices have also developed a handheld mass spectrometer based on a CIT (M908 [275]), and the Sam Yang Chemical company has developed a similar 'palm portable' system [276]. Toroidal traps have been developed at Brigham Young University [277] and commercialized at Torion, now partnered with Smiths Detection. Both have products for homeland security applications (Tridion-9 [278] and Guardion [279]).

Microsaic have developed the portable Chempack™ instrument containing MEMS [280], related to the previously described Chemcube™. Figure 18(a) shows the instrument,
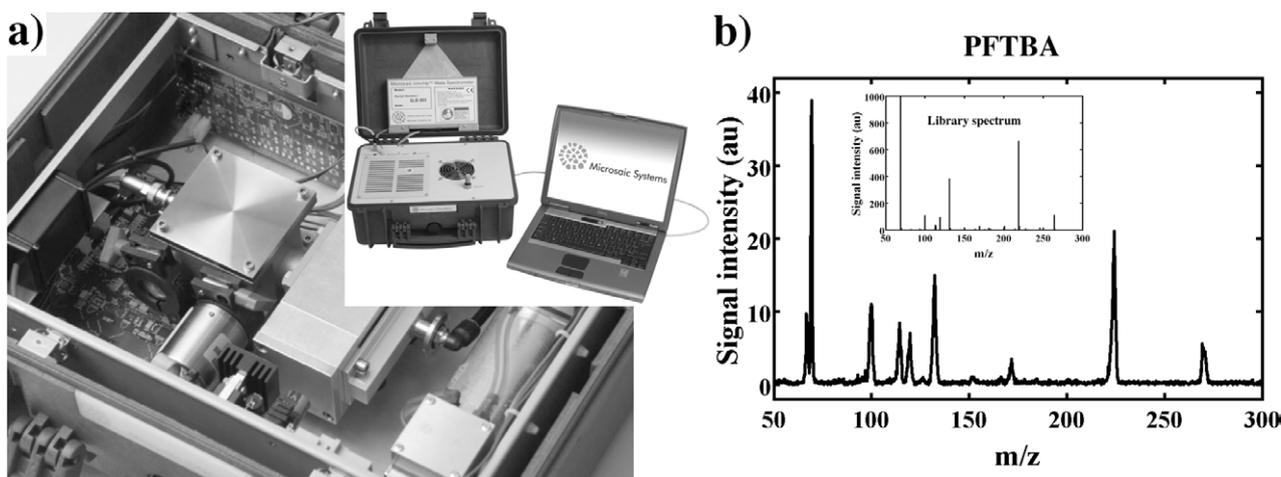
Figure 18. Portable MEMS mass spectrometer: (a) Chempack™ instrument (courtesy Microsaic Systems) and (b) mass spectrum of perfluorotributylamine (courtesy Microsaic Systems, reprinted with permission from Malcolm A *et al* 2010 *Anal. Chem.* **82** 1751–8 [207]. Copyright 2010 American Chemical Society).

which had a weight of 15 kg, a pump-down time of 5 min, a Li ion battery pack with a life of 10 h, and a mass range of $m/z = 400$. Figure 18(b) compares the measured spectrum of perfluorotributylamine (PFTBA) and the corresponding library spectrum, showing good performance up to $m/z = 250$.

7.2. Security applications

The rising incidence of terror attacks and asymmetric warfare have accelerated development of portable MS for the detection of explosives, and potentially large markets exist for passenger screening in transport hubs. Unfortunately, most nitrogen-based explosives have very low vapor pressure [281]. Although considerable advances have been made in portable MS for explosive detection [282–284], improvements in sensitivity are still required.

Preconcentrators (which adsorb explosive molecules onto chemoselective surfaces [285, 286], and then thermally desorb them in a concentrated pulse) are used to improve detection limits. Here, MEMS have again made a significant contribution. The ability of integrated systems to reduce dead volumes has increased concentration factors, while the low thermal mass of miniaturized parts has decreased cycle times. Two variants have been developed: valved systems (which alternately expose the chemoselective surface to ambient atmosphere and then to the analysis system) [287–291], and flow-through systems (which rely purely on cyclic heating) [292–295]. Of these, the best known is CASPAR (Cascade Avalanche Sorbent Plate aRray), developed at NRL [292].

Searches for weapons of mass destruction have similarly spurred development of MS methods for detecting chemical weapons such as mustard gas and sarin [296]. Field-portable GC-MS systems have been demonstrated [297, 298], and the MEMS TOF-MS under development at LETI-DAM is targeted at similar applications [299]. However, the limited mass range of small MS systems has made it difficult to detect biological weapons such as anthrax. Law enforcement applications include the detection of recreational drugs [300, 301],

and forensic detection of drug metabolites in blood, hair or fingerprints and accelerants at fire scenes [302, 303]. Related applications include the detection of performance enhancing drugs in sports.

7.3. Industrial and medical applications

The oldest applications for portable MS are leak detection (originally developed by Nier during the Manhattan project [304]) and residual gas analysis. Many suitable systems are commercially available, often based on quadrupole filters [128]. Current industrial applications requiring portability include the monitoring of oil spills [305] and wastewater from oil sand [306], the measurement of gas and water in borehole fluids [307, 308] and analysis of downhole fluids for reservoir evaluation [309]. Benchtop MS systems for general industrial analysis containing EI sources and miniature mass filters have again been developed (e.g. 1st Detect MMS-1000; cylindrical trap [310]).

The use of miniature MS in pharmaceutical labs is a growing application. Typically, chemists confirm that a reaction has produced the desired product by submitting samples to a centralized, queued-access LC-MS facility. Workflows can be improved and delays minimized using a small, low-cost ESI instrument in the lab itself. High sensitivities are not required as samples normally have mg ml^{-1} concentration. Compact conventional systems are available (e.g. Advion Expression CMS; quadrupole [311]), and MEMS-based systems (the 3500MiD and 4000MiD) have again been developed by Microsaic. These instruments can be coupled to LC systems [11, 312]. Figure 19(a) shows the total ion chromatogram (TIC) and base peak chromatogram (BPC) obtained using the 3500 MiD coupled to conventional HPLC. Each peak corresponds to elution of a component of an injected mixture (here, melamine, reserpine, warfarin and simvastin). Figure 19(b) shows the mass spectrum corresponding to the reserpine peak at a retention time of 5.7 min.

Alternatively, miniature mass spectrometers can be used for automated on-line monitoring of reactions [313, 314]. Small samples are periodically withdrawn, diluted and
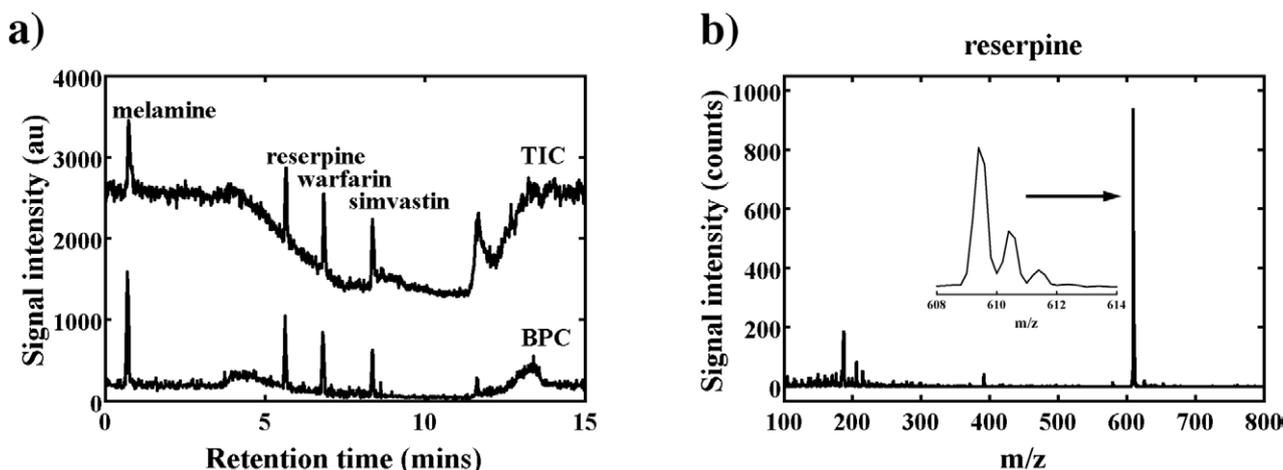
Figure 19. Performance of MEMS ESI-MS: (a) total ion chromatogram (TIC) and base peak chromatogram (BPC) for a multi-component LC separation; (b) mass spectrum corresponding to the reserpine peak reproduced with permission from Malcolm A *et al* 2011 *Rapid Comm. Mass Spectrom.* **25** 3281–8 [11] (courtesy Microsaic Systems; copyright © John Wiley & Sons, Ltd).

then directly analysed without chromatographic separation Reaction conditions can be quickly optimized this way and unstable compounds that would decompose during an LC-MS analysis can be monitored.

The oldest medical applications of portable MS include monitoring of anaesthesia [315, 316] and of respiration in artificially ventilated intensive-care patients [317], and the detection of breath markers for lung cancer [318]. More recent applications include cancer diagnosis by analysis of vapors generated during radiofrequency electrosurgery [319]. New sampling techniques such DESI are being used to differentiate normal tissue from cancerous tissue in biopsy samples [320], in some cases during endoscopic procedures (by sealing the sampling probe directly against the tissue, and transferring the desorbed charged species along a tube) [321]. Other recent medical applications include the detection of bacterial infections such as strep throat from swabs [322].

7.4. Environmental and consumer protection applications

Environmental applications involve the monitoring of pollution in the air, soil, and waterways. Man-made pollutants include vehicle exhaust, toxic emissions from process plants and greenhouse gases, while more 'natural' pollutants include toxic algae encouraged by global warming. Portable, hand-held and backpack-mounted instruments have been used to monitoring atmospheric pollutants, in some cases autonomously [323–326]. Instruments have been mounted in submersibles with membrane inlets for measurement of dissolved gases and volatile organics in seawater [327, 328], and flown in light aircraft to detect emissions from active volcanoes [329, 330].

Consumer protection applications include the detection of counterfeit medical drugs [331] and adulterants in food, including herbicide and pesticide residues, antibiotics and veterinary drugs, carcinogenic dyes, preservatives and other illegal additives [332–334]. Appropriate conventional and portable MS monitoring is being developed [335, 336]. However, the specificity and sensitivity typically requires

tandem mass spectrometry. Tandem MS has been demonstrated using miniaturized LITs, which allow the operations of ion selection, fragmentation and analysis to be carried out in sequence in the same component [337]. Microsaic have developed a MEMS-based tandem-MS system in the form of a triple quadrupole [209], which carries out MS-MS as 'tandem in space' rather than 'tandem in time'.

7.5. General scientific applications

A significant scientific application of portable mass spectrometers continues to be space exploration. In unmanned probes, these have historically been used for characterization of the upper atmosphere, space plasmas, interstellar dust, and planetary and cometary atmospheres [338–340]. More recent unmanned landers and planetary rovers have included GC-MS for analysis of thermally evolved gas [341] or laser ablation ionization for elemental and isotopic analysis of rocks [342, 343]. A strong driver is the search for organic molecules that might indicate an extraterrestrial origin of life. Manned flights such as the NASA Space Shuttle have additionally used mass spectrometers for monitoring of cabin air and water quality [232, 344]. A number of space-borne systems have already used MEMS [73, 105, 106, 127] and this trend looks set to continue in low-cost missions [345] and miniaturized satellites such as CubeSat [346].

More recently, there has been interest in chip-scale ion trap arrays for quantum information processing [347–349]. In this case, the emphasis is on creating, transporting and confining ion packets based on ionized single atoms, which are deliberately injected, rather than chemical analysis of larger, unknown molecules. Much lower selectivity and mass range are therefore required; instead, it is the ability to interact selected numbers of ions with observable quantities such as spin (known as 'qubits') to perform quantum computational operations that is important. The amount of information held by such a system scales as 2^N, where N is the number of qubits, and hence may rapidly outrun the capability of conventional electronic processors.
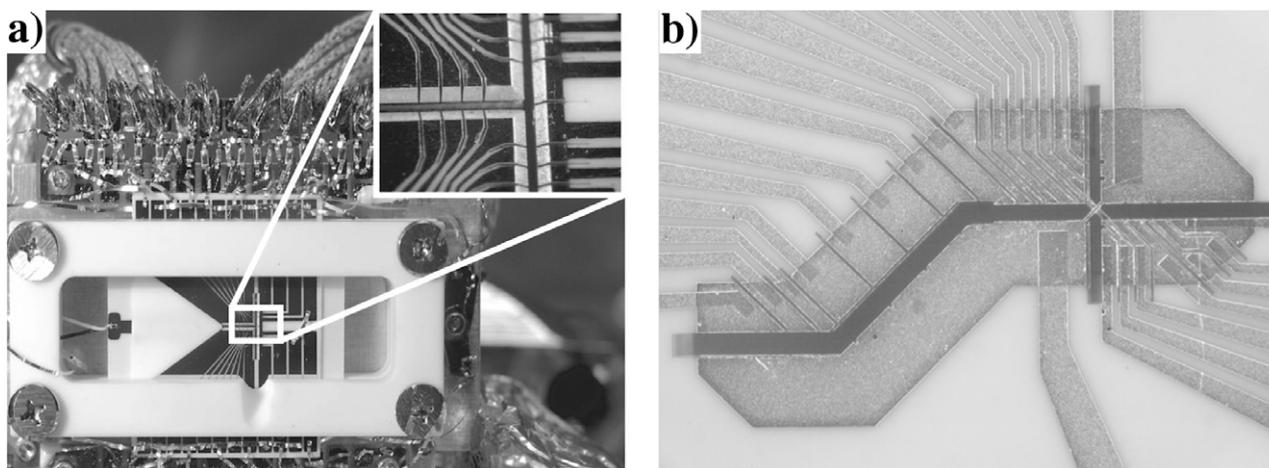
Figure 20. Microfabricated quantum processors: (a) T-junction ion guide (courtesy Professor Winfried Hensinger, Sussex University; reproduced by permission from Hensinger *et al* 2006 *Appl. Phys. Lett.* **88** 034101 [351]. Copyright 2006, AIP Publishing LLC); (b) X-junction ion guide (courtesy Dr Brad Blakestad, California Institute of Technology).

Silicon-based linear ion trap arrays [350] and sophisticated ion optical circuits such as T-junctions [351] and X-junctions [352] have now been demonstrated, in each case based on the surface electrode approximation. Figures 20(a) and (b) show T- and X-junctions, respectively. The same problems (RF heating, and flashover at high voltage) in devices with poor electrical isolation have been observed [353]. However these are now being overcome using Si_3N_4 isolation layers in place of SiO_2 [354, 355]. Development seems to be following a similar path to MEMS MS, and the advantage of MEMS in realizing complex functionality and reducing coupling losses is clear.

8. Opportunities and challenges

MEMS MS has advanced considerably. Performance is now good enough to enable applications requiring portability, small size or low cost. The availability of such systems – which allow the instrument to be taken to the sample—now allows *in situ* analysis. Mainframe instruments are evolving into desktop systems, backpack-mounted systems into hand-held units, and vehicle-mounted systems into airborne systems. The new paradigm will generate changes broadly analogous to those driven by the development of personal computers. However, many opportunities and challenges remain.

The most promising commercial opportunities are those for which compact instruments with moderate performance are required in significant numbers. Unfortunately, the original drivers do not satisfy all these constraints. For example, although lightweight instruments are needed for space exploration, the market is drastically limited. Similarly, although portable instruments are required in large numbers for explosives detection, achieving sufficient sensitivity is challenging. Some important laboratory applications (high-throughput analysis for proteomics and metabolomics) remain similarly out of reach, because of limitations on mass range. However, on-line monitoring of chemical synthesis and food safety are both suitable applications. Success in these markets should

allow other applications, and foster the performance improvements needed.

The most significant challenge for MEMS MS is that miniaturizing components such as sources and filters has relatively little impact on overall cost. The two largest contributors to the overall cost of manufacturing are assembly and alignment of the ion optical system, and the vacuum pumps. Nevertheless, recent developments have shown that investment in MEMS can pay dividends, since its ability to provide precision alignment can reduce assembly costs, and provision of sub-components as packaged modules can reduce downtime and the lifetime costs of servicing. The cost of conventional pumps will clearly reduce as volumes rise. As a result, MEMS MS should address some markets at costs that cannot be matched by conventional instruments.

If the performance and reliability of MEMS MS can be improved and sizes reduced, significant gains may be achieved. Systems based on integrated vacuum chambers and MEMS-based pumps would open new markets for hand-held instruments. The ability of a mass spectrometer to act as a universal gas sensor would then allow replacement of dedicated chemical sensors, with applications ranging from engine emission monitoring to point-of-care diagnosis of cancer and hazard detection. In the latter case, a key advance would be to move beyond the restriction of passenger screening to choke points in transportation hubs. MEMS MS may therefore be poised to address many of today's major societal challenges, including the environment, health and security.

Acknowledgments

References

[1] Petersen K E 1982 Silicon as a mechanical material *Proc. IEEE* **70** 420–57

[2] Howe R T *et al* 1990 Silicon micromechanics: sensors and actuators on a chip *IEEE Spectrum* **27** 29–31

[3] Fujita H 1998 Microactuators and micromachines *Proc. IEEE* **86** 1721–32

[4] Judy J W 2001 Microelectromechanical systems (MEMS): fabrication, design and applications *Smart Mater. Struct.* **10** 1115–34

[5] Madou M J 2011 *Fundamentals of Microfabrication and Nanotechnology* 3rd edn (Boca Raton, FL: CRC Press)

[6] van den Berg A and Lammerink T S J 1998 Micro total analysis systems: microfluidic aspects, integration concept and applications *Microsystem Technology in Chemistry and Life Science* ed A Manz and H Becker (Berlin: Springer) pp 21–49

[7] Manz A, Graber N and Widmer H M 1990 Miniaturized total chemical analysis systems: a novel concept for chemical sensing *Sensors Actuators* B **1** 244–8

[8] Dittrich P S, Tachikawa K and Manz A 2006 Micro total analysis systems. Latest advancements and trends *Anal. Chem.* **78** 3887–908

[9] Culbertson C T *et al* 2014 Micro total analysis systems: fundamental advances and biological applications *Anal. Chem.* **86** 95–118

[10] Taylor S *et al* 2000 Quadrupole mass spectrometers *US Patent Specification* 6025591

[11] Malcolm A *et al* 2011 A miniature mass spectrometer for liquid chromatography applications *Rapid Commun. Mass Spectrom.* **25** 3281–8

[12] Dawson P H, Hedman J W and Whetten N R 1970 A miniature mass spectrometer *Anal. Chem.* **42** 103A–8A

[13] Nier A O and Hayden J L 1971 A miniature Mattauch–Herzog mass spectrometer for the investigation of planetary atmospheres *Int. J. Mass Spectrom. Ion Phys.* **6** 339–46

[14] Bailey C A, Kilvington J and Robinson N W 1971 A miniature time of flight mass spectrometer *Vacuum* **21** 461–74

[15] De Hoffmann E, Charette J and Stroobant V 1996 *Mass Spectrometry: Principles and Applications* (Chichester: Wiley)

[16] Sinha M P and Tomassian A D 1991 Development of a miniaturized, lightweight magnetic-sector for a field-portable mass spectrograph *Rev. Sci. Instrum.* **62** 2618–20

[17] Diaz J A, Giese C F and Gentry W R 2001 Sub-miniature $E \times B$ sector-field mass spectrometer *J. Am. Soc. Mass Spectrom.* **12** 619–32

[18] Cornish T J and Bryden W A 1999 Miniature time-of-flight mass spectrometer for a field-portable biodetection system *Johns Hopkins APL Tech. Dig.* 20 335–42

[19] Cornish T J, Ecelberger S and Brinckerhoff W 2000 Miniature time-of-flight mass spectrometer using a flexible circuitboard reflector *Rapid Commun. Mass Spectrom.* **14** 2408–11

[20] Ferran R J and Boumsellek S 1996 High-pressure effects in miniature arrays of quadrupole analyzers for residual gas analysis from 10^{-9} to 10^{-2} Torr *J. Vac. Sci. Technol.* A **14** 1258–64

[21] Boumsellek S and Ferran R J 2001 Tradeoffs in miniature quadrupole designs *J. Am. Soc. Mass Spectrom.* **12** 633–40

[22] Orient O J, Chutjian A and Garkanian V 1997 Miniature, high-resolution, quadrupole mass-spectrometer array *Rev. Sci. Instrum.* **68** 1393–7

[23] Wu G, Cooks R G and Ouyang Z 2005 Geometry optimization for the cylindrical ion trap: field calculations, simulations and experiments *Int. J. Mass Spectrom.* **241** 119–32

[24] Badman E R and Cooks R G 2000 A parallel miniature cylindrical ion trap array *Anal. Chem.* **72** 3291–7

[25] Badman E R and Cooks R G 2000 Cylindrical ion trap array with mass selection by variation in trap dimensions *Anal. Chem.* **72** 5079–86

[26] Ouyang Z *et al* 2004 Rectilinear ion trap: concepts, calculations, and analytical performance of a new mass analyzer *Anal. Chem.* **76** 4595–605

[27] Fico M *et al* 2007 Miniaturization and geometry optimization of a polymer-based rectilinear ion trap *Anal. Chem.* **79** 8076–82

[28] Clare A T *et al* 2010 Linear ion trap fabricated using rapid manufacturing technology *J. Am. Soc. Mass Spectrom.* **21** 317–22

[29] Badman E R and Cooks R G 2000 Special feature: perspective—miniature mass analysers *J. Mass. Spectrom.* **35** 659–71

[30] Ouyang Z and Cooks R G 2009 Miniature mass spectrometers *Annu. Rev. Anal. Chem.* **2** 187–214

[31] Kovacs G T A, Maluf N I and Petersen K E 1998 Bulk micromachining of silicon *Proc. IEEE* **86** 1536–51

[32] Bustillo J M, Howe R T and Muller R S 1998 Surface micromachining for microelectromechanical systems *Proc. IEEE* **86** 1552–74

[33] Guckel H 1998 High-aspect-ratio micromachining via deep x-ray lithography *Proc. IEEE* **86** 1586–93

[34] Lorenz H *et al* 1997 SU-8: a low-cost negative resist for MEMS *J. Micromech. Microeng.* **7** 121–4

[35] Jansen H *et al* 1996 A survey on the reactive ion etching of silicon in microtechnology *J. Micromech. Microeng.* **6** 14–28

[36] Laermer F and Schilp A 1996 Method of anisotropically etching silicon *US Patent Specification* 5501893

[37] Bhardwaj J K and Ashraf H 1995 Advanced silicon etching using high-density plasmas *Proc. SPIE* **2639** 224–33

[38] Klaassen E H *et al* 1996 Silicon fusion bonding and deep reactive ion etching: a new technology for microstructures *Sensors Actuators* A **52** 132–9

[39] Schmidt M A 1998 Wafer-to-wafer bonding for microstructure formation *Proc. IEEE* **86** 1575–85

[40] Yan X and Gu P 1996 A review of rapid prototyping technologies and systems *Comput. Aided Design* **28** 307–18

[41] Noorani R 2006 *Rapid Prototyping: Principles and Applications* (Hoboken, NJ: Wiley)

[42] Bertsch A, Lorenz H and Renaud P 1999 3D microfabrication by combining microstereolithography and thick resist UV lithography *Sensors Actuators* A **73** 14–23

[43] SIMION® Version 8.1 (http://simion.com)

[44] Syms R R A 2009 Advances in microfabricated mass spectrometers *Anal. Bioanal. Chem.* **393** 427–9

[45] Sikanen T *et al* 2010 Microchip technology in mass spectrometry *Mass Spectrom. Rev.* **29** 351–91

[46] Arscott S 2014 SU-8 as a material for lab-on-a-chip-based mass spectrometry *Lab Chip* **14** 3668–89

[47] Syms R R A 2015 Status and future trends of the miniaturization of mass spectrometry *IEEE MEMS. Conf. (Estoril, Portugal, 18–22 January 2015)* pp 134–9

[48] Brown I G 2004 *The Physics and Technology of Ion Sources* 2nd edn (Weinheim: Wiley)

[49] Gomer R 1961 *Field Emission and Field Ionization* (Cambridge, MA: Harvard University Press)

[50] Jarvis K E, Gray A L, Houk R S 1992 *Handbook of Inductively Coupled Plasma Mass Spectrometry)* (London: Blackie Academic and Professional)

[51] Marr G V 1967 *Photoionization Processes in Gases)* (New York: Academic)

[52] Vertes A, Gijbels R and Adams F 1993 *Laser Ionization Mass Analysis* (New York: Wiley)

[53] Hillenkamp F, Peter-Katalinic J 2007 *MALDI MS: a Practical Guide to Instrumentation, Methods and Applications* (Weinheim: Wiley-VCH)

[54] Cole R B 1997 *Electrospray Ionization Mass Spectrometry: Fundamentals, Instrumentation and Applications* (New York: Wiley)

[55] Wilm M 2011 Principles of electrospray ionization *Mol. Cell. Proteomics* **10** M111.009407

[56] Taylor G I 1964 Disintegration of water drops in an electric field *Proc. R. Soc. Lond.* A **280** 383–97

[57] Gale D C and Smith R D 1993 Small volume and low flow-rate electrospray ionization mass spectrometry of aqueous samples *Rapid Commun. Mass Spectrom.* **7** 1017–21

[58] Wilm M and Mann M 1996 Analytical properties of the nanoelectrospray ion source *Anal. Chem.* **68** 1–8

[59] Takáts Z *et al* 2004 Mass spectrometry sampling under ambient conditions with desorption electrospray ionization *Science* **306** 471–3

[60] Gao L, Cooks R G and Ouyang Z 2008 Breaking the pumping speed barrier in mass spectrometry: discontinuous atmospheric pressure interface *Anal. Chem.* **80** 4026–32

[61] Pawliszyn J 2012 *Handbook of Solid Phase Microextraction* (London: Elsevier)

[62] Johnson R C *et al* 2000 Membrane introduction mass spectrometry: trends and applications *Mass Spectrom. Rev.* **19** 1–37

[63] Yamashita M and Fenn J B 1984 Electrospray ion source. Another variation on the free-jet theme *J. Phys. Chem.* **88** 4451–9

[64] Zhou L *et al* 2003 Incorporation of a Venturi device in electrospray ionization *Anal. Chem.* **75** 5978–83

[65] Shaffer S A *et al* 1997 A novel ion funnel for focusing ions at elevated pressure using electrospray ionization mass spectrometry *Rapid Commun. Mass Spectrom.* **11** 1813–7

[66] Yoon H J *et al* 2001 The test of hot emission for the micro mass spectrometer *Proc. SPIE* **4408** 360–7

[67] Yoon H J *et al* 2007 Fabrication of two types of micro ion sources for a micro time-of-flight mass spectrometer *J. Micromech. Microeng.* **17** 1542–8

[68] Tassetti C-M *et al* 2013 A MEMS electron impact ion source integrated in a micro time-of-flight mass spectrometer *Sensors Actuators* B **189** 173–8

[69] Marcus R B *et al* 1990 Formation of silicon tips with <1 nm radius *Appl. Phys. Lett.* **56** 236–8

[70] She J C *et al* 1999 Comparative study of electron emission characteristics of silicon tip arrays with and without amorphous diamond coating *J. Vac. Sci. Technol.* B **17** 592–5

[71] Felter T E 1999 Cold cathode field emitter array on a quadrupole mass spectrometer: route to miniaturization *J. Vac. Sci Technol.* B **17** 1993–6

[72] Kornienko O *et al* 2000 Field-emission cold-cathode EI source for a microscale ion trap mass spectrometer *Anal. Chem.* **72** 559–62

[73] Huq S E *et al* 2001 Field emitters for space application *J. Vac. Sci. Technol.* B **19** 988–91

[74] Yoon H J *et al* 2007 Fabrication of an ion source using carbon nanoparticle field emitters for a micro time-of-flight mass spectrometer *Proc. Transducers Conf. (Lyon, France*, *10–14 June 2007)* pp 1067–70

[75] Bower C A *et al* 2007 On-chip electron-impact ion source using carbon nanotube field emitters *Appl. Phys. Lett.* **90** 124102

[76] Han K *et al* 2011 Field emission ion source using a carbon nanotube array for micro time-of-flight mass spectrometer *Japan. J. Appl. Phys.* **50** 06GM04

[77] Chen L-Y *et al* 2011 A microionizer for portable mass spectrometers using double-gated isolated vertically aligned carbon nanofibers arrays *IEEE Trans. Electron Devices* **58** 2149–58

[78] Syage J A, Hanning-Lee M A and Hanold K A 2000 A man-portable, photoionization time-of-flight mass spectrometer *Field Anal. Chem. Technol.* **4** 204–15

[79] Haapala M *et al* 2007 Microchip for combining gas chromatography or capillary liquid chromatography with atmospheric pressure photoionization-mass spectrometry *Anal. Chem.* **79** 4994–9

[80] Haapala M, Suominen T and Kostiainen R 2013 Capillary photoionization: a high sensitivity ionization method for mass spectrometry *Anal. Chem.* **85** 5715–9

[81] Frame J W *et al* 1997 Microdischarge devices fabricated in silicon *Appl. Phys. Lett.* **71** 1165–7

[82] Hopwood J A 2000 A microfabricated inductively coupled plasma generator *J. Microelectromech. Syst.* **9** 309–13

[83] Bass A, Chevalier C and Blades M W 2001 A capacitively coupled microplasma (CCμP) formed in a channel in a quartz wafer *J. Anal. At. Spectrom.* **16** 919–21

[84] Longwitz R G, van Lintel H and Renaud P 2003 Study of micro-glow discharges as ion sources for ion mobility spectrometry *J. Vac. Sci. Technol.* B **21** 1570–3

[85] Hopwood J *et al* 2005 A microfabricated atmospheric-pressure microplasma source operating in air *J. Phys. D. Appl. Phys.* **38** 1698–703

[86] Siebert P *et al* 1998 Surface microstructure/miniature mass spectrometer: processing and applications *Appl. Phys.* A **67** 155–60

[87] Limbach P A and Meng Z 2002 Integrating micromachined devices with modern mass spectrometry *Analyst* **127** 693–700

[88] Sung W-C, Makamba H and Chen S-H 2005 Chip-based microfluidic devices coupled with electrospray ionization-mass spectrometry *Electrophoresis* **26** 1783–91

[89] Lazar I M, Grym J and Foret F 2006 Microfabricated devices: a new sample introduction approach to mass spectrometry *Mass Spectrom. Rev.* **25** 573–94

[90] Koster S and Verpoorte E 2007 A decade of microfluidic analysis coupled with electrospray mass spectrometry: an overview *Lab. Chip* **7** 1394–412

[91] Chiarot P R, Sullivan P and Ben Mrad R 2011 An overview of electrospray applications in MEMS and microfluidic systems *J. Microelectromech. Syst.* **20** 1241–9

[92] Ramsey R S and Ramsey J M 1997 Generating electrospray from microchip devices using electroosmotic pumping *Anal. Chem.* **69** 1174–8

[93] Licklider L *et al* 2000 A micromachined chip-based electrospray source for mass spectrometry *Anal Chem.* **72** 367–75

[94] Le Gac S *et al* 2003 2D microfabricated sources for nanoelectrospray *J. Mass Spectrom.* **38** 1259–64

[95] Arscott S *et al* 2004 A planar on-chip micro-nib interface for nanoESI–MS microfluidic applications *J. Micromech. Microeng.* **14** 310–6

[96] Arscott S, Legrand B, Buchaillot L and Ashcroft A E 2007 A silicon beam-based microcantilever nanosprayer *Sensors Actuators* B **125** 72–8

[97] Nissilä T *et al* 2007 Silicon micropillar array electrospray chip for drug and biomolecule analysis *Rapid Commun. Mass Spectrom.* **21** 3677–82

[98] Wang H *et al* 2010 Paper spray for direct analysis of complex mixtures using mass spectrometry *Angew. Chem.* **122** 889–92

[99] Xue Q *et al* 1997 Multichannel microchip electrospray mass spectrometry *Anal. Chem.* **69** 426–30

[100] Schultz G A *et al* 2000 A fully integrated monolithic microchip electrospray device for mass spectrometry *Anal. Chem.* **72** 4058–63

[101] Griss P *et al* 2002 Development of micromachined hollow tips for protein analysis based on nanoelectrospray

ionization mass spectrometry *J. Micromech. Microeng.* **12** 682–7

[102] Zhang S, Van Pelt C K and Henion J D 2003 Automated chip-based nano-electrospray mass spectrometry for the rapid identification of proteins separated by 2D gel electrophoresis *Electrophoresis* **24** 3620–2

[103] Syms R R A *et al* 2007 A microengineered alignment bench for a nanospray ionization source *J. Micromech. Microeng.* **17** 1567–74

[104] Jurcicek P, Zou H and Gao S 2013 Design, simulation and fabrication of a MEMS-based air amplifier for electrospray ionization *J. Micro/Nanolithogr. MEMS MOEMS* **12** 023006

[105] Jamieson B G *et al* 2007 Microfabricated silicon leak for sampling planetary atmospheres with a mass spectrometer *Rev. Sci. Instrum.* **78** 065109

[106] Roman P A *et al* 2008 A miniature MEMS and NEMS enabled time-of-flight mass spectrometer for investigations in planetary science *Proc. SPIE* **6959** 69590G

[107] Wright S *et al* 2010 MEMS-based nanospray ionization mass spectrometer *J. Microelectromech. Syst.* **19** 1430–43

[108] Chaudhary A, van Amerom F H W and Short R T 2014 A novel planar ion funnel design for miniature ion optics *Rev. Sci. Instrum.* **85** 105101

[109] Anthony S N, Shinholt D L and Jarrold M F 2014 A simple electrospray interface based on a DC ion carpet *Int. J. Mass Spectrom.* **371** 1–7

[110] Griffiths J 2008 A brief history of mass spectrometry *Anal. Chem.* **80** 5678–83

[111] Yates J R 2011 A century of mass spectrometry: from atoms to proteomes *Nature Methods* **8** 633–7

[112] Sharma K S 2013 Mass spectrometry—the early years *Int. J. Mass Spectrom.* **349-50** 3–8

[113] Münzenberg G 2013 Development of mass spectrometers from Thomson and Aston to present *Int. J. Mass Spectrom.* **349–50** 9–18

[114] Duckworth H E 1958 *Mass Spectroscopy* (Cambridge: Cambridge University Press)

[115] Aberth W and Wollnick H 1990 The Wien filter and its application in chemistry *Mass Spectrom. Rev.* **9** 383–404

[116] Freidhoff C B, Young R M and Sriram S 1995 Solid state micro-machined mass spectrograph universal gas detection sensor *US Patent Specification* 5386115

[117] Freidhoff C B *et al* 1999 Chemical sensing using non-optical microelectromechanical systems *J. Vac. Sci. Technol.* A **17** 2300–7

[118] Sillon N and Baptist R 2002 Micromachined mass spectrometer *Sensors Actuators* B **83** 129–37

[119] Gilchrist K H *et al* 2007 A novel ion source and detector for a miniature mass spectrometer *Proc. IEEE Sensors Conf. (Atlanta, GA, 28–31 October 2007)* pp 1372–5

[120] Russell Z E *et al* 2015 2D aperture coding for magnetic sector mass spectrometry *J. Am. Soc. Mass Spectrom.* **26** 248–56

[121] Chen E X *et al* 2015 Order of magnitude signal gain in magnetic sector mass spectrometry via aperture coding *J. Am. Soc. Mass Spectrom.* **26** 1633–40

[122] Cotter R J 1997 *Time-of-Flight Mass Spectrometry: Instrumentation and Applications in Biological Research* (Washington, DC: ACS Publications)

[123] Yoon H J *et al* 2002 Fabrication of a novel micro time-of-flight mass spectrometer *Sensors Actuators* A **97–8** 441–7

[124] Tassetti C-M *et al* 2013 Gas detection and identification using MEMS TOF mass spectrometer *Proc. Transducers Conf. (Barcelona, Spain, 16–20 June 2013)* pp 1162–5

[125] Fox J *et al* 2009 Microelectromechanical system assembled ion optics: an advance to miniaturization and assembly of electron and ion optics *Rev. Sci. Instrum.* **80** 093302

[126] Wapelhorst E, Hauschild J-P and Müller J 2007 Complex MEMS: a fully integrated TOF micro mass spectrometer *Sensors Actuators* A **138** 22–7

[127] Brinkfelt K *et al* 2010 Microshutters for space physics time-of-flight applications *Proc. Micromechanics and Microsystems Workshop (Enschede, The Netherlands, 26–29 September 2010)* pp 140–3

[128] Dawson P H 1976 *Quadrupole Mass Spectrometry and its Applications* (Amsterdam: Elsevier)

[129] March R E and Todd J F 2005 *Quadrupole Ion Trap Mass Spectrometry* 2nd edn (Hoboken, NJ: Wiley)

[130] McLafferty F W 1983 *Tandem Mass Spectrometry* (New York: Wiley)

[131] Zubarev R A and Makarov A 2013 Orbitrap mass spectrometry *Anal. Chem.* **85** 5288–96

[132] Zhang Z *et al* 2009 Paul trap mass analyzer consisting of opposing microfabricated electrode plates *Anal. Chem.* **81** 5241–8

[133] Li A *et al* 2014 Miniaturization of a planar-electrode linear ion trap mass spectrometer *Rapid Commun. Mass Spectrom.* **28** 1338–44

[134] Austin D E *et al* 2007 Halo ion trap mass spectrometer *Anal. Chem.* **79** 2927–32

[135] Wang M J *et al* 2011 Performance of a halo ion trap mass analyzer with exit slits for axial ejection *J. Am. Soc. Mass Spectrom.* **22** 369–78

[136] Wiberg D V *et al* 2003 LIGA-fabricated 2D quadrupole array and scroll pump for miniature gas chromatograph/mass spectrometer *Proc. SPIE* **4878** 8–13

[137] Velásquez-García L F, Cheung K and Akinwande A I 2008 An application of 3-D MEMS packaging: out-of-plane quadrupole filters *J. Microelectromech. Syst.* **17** 1430–8

[138] Syms R R A *et al* 1996 Fabrication of a microengineered electrostatic quadrupole lens *Elect. Lett.* **32** 2094–5

[139] Syms R R A *et al* 1998 Design of a microengineered quadrupole electrostatic lens *IEEE Trans. Electron Devices* **45** 2304–11

[140] Taylor S *et al* 1998 Initial results for a quadrupole mass spectrometer with a silicon micromachined mass filter *Electron. Lett.* **34** 546–7

[141] Taylor S *et al* 1999 Performance improvements for a miniature quadrupole with a micromachined mass filter *Vacuum* **53** 203–6

[142] Syms R R A, Michelutti L and Ahmad M M 2003 2D microfabricated electrostatic einzel lens *Sensors Actuators* A **107** 285–95

[143] Geear M *et al* 2005 Monolithic MEMS quadrupole mass spectrometers by deep silicon etching *J. Microelectromech. Syst.* **14** 1156–66

[144] Wright S *et al* 2010 Microfabricated quadrupole mass spectrometer with a Brubaker prefilter *J. Microelectromech. Syst.* **19** 325–37

[145] Cheung K, Velásquez-García L F and Akinwande A I 2010 Chip-scale quadrupole mass filters for portable mass spectrometry *J. Microelectromech. Syst.* **19** 469–83

[146] Hogan T J *et al* 2010 Performance characteristics of a MEMS quadrupole mass filter with square electrodes: experimental and simulated results *IEEE Trans. Inst. Meas.* **59** 2458–66

[147] Madsen M J *et al* 2004 Planar ion trap geometry for microfabrication *Appl. Phys.* B **78** 639–51

[148] Stick D *et al* 2006 Ion trap in a semiconductor chip *Nat. Phys.* **2** 36–9

[149] Brewer R G, DeVoe R G and Kallenbach R 1992 Planar ion microtraps *Phys. Rev.* A **46** R6781–4

[150] Kornienko O *et al* 1999 Micro ion trap mass spectrometry *Rapid Commun. Mass Spectrom.* **13** 50–3

[151] Chaudhary A *et al* 2006 Fabrication and testing of a miniature cylindrical ion trap mass spectrometer

constructed from low temperature co-fired ceramics *Int. J. Mass Spectrom.* **251** 32–9

[152] Pau S *et al* 2006 Microfabricated quadrupole ion trap for mass spectrometer applications *Phys. Rev. Lett.* **96** 120801

[153] van Amerom F H W *et al* 2007 Microfabrication of cylindrical ion trap mass spectrometer arrays for handheld chemical analyzers *Chem. Eng. Commun.* **195** 98–114

[154] Chaudhary A, van Amerom F H W and Short R T 2009 Development of microfabricated cylindrical ion trap mass spectrometer arrays *J. Microelectromech. Syst.* **18** 442–8

[155] Blain M G *et al* 2004 Towards the hand-held mass spectrometer: design considerations, simulation, and fabrication of micrometer-scaled cylindrical ion traps *Int. J. Mass Spectrom.* **236** 91–104

[156] Darling R B *et al* 2002 Micromachined Faraday cup array using deep reactive ion etching *Sensors Actuators* A **95** 84–93

[157] Scheidemann A A *et al* 2002 Faraday cup detector array with electronic multiplexing for multichannel mass spectrometry *J. Vac. Sci. Technol.* A **20** 597–604

[158] Bower C A *et al* 2007 Microfabrication of fine-pitch high aspect ratio Faraday cup arrays in silicon *Sensors Actuators* A **137** 296–301

[159] Sinha M P and Wadsworth M 2005 Miniature focal plane mass spectrometer with 1000-pixel modified-CCD detector array for direct ion measurement *Rev. Sci. Instrum.* **76** 025103

[160] Shank S M *et al* 1995 Fabrication of high aspect ratio structures for microchannel plates *J. Vac. Sci. Technol.* B **13** 2736–40

[161] Beetz C P *et al* 2000 Silicon-micromachined microchannel plates *Nucl. Instrum. Methods Phys. Res.* A **442** 443–51

[162] Tremsin A S *et al* 2003 The latest developments of high gain Si microchannel plates *Proc. SPIE* **4854** 215–24

[163] Birkinshaw K and Langstaff D P 1994 Silicon technology in ion detection—a high resolution detector array *Int. J. Mass Spectrom. Ion Process.* **132** 193–206

[164] Vickers J S and Chakrabarti S 1999 Silicon-anode detector with integrated electronics for microchannel-plate imaging detectors *Rev. Sci. Instrum.* **70** 2912–6

[165] Hadjar O *et al* 2012 Preliminary demonstration of an IonCCD as an alternative pixelated anode for direct MCP readout in a compact MS-based detector *J. Am. Soc. Mass Spectrom.* **23** 418–24

[166] Kawarabayashi J *et al* 1998 Development of a micro array type electron multiplier *IEEE Trans. Nucl. Sci.* **45** 568–71

[167] Inoue M *et al* 2000 Development of a new position sensitive electron multiplication device fabricated by LIGA process *Microsyst. Technol.* **6** 90–3

[168] Ono T and Esashi M 2005 Stress-induced mass detection with a micromechanical/ nanomechanical silicon resonator *Rev. Sci. Instrum.* **76** 093107

[169] Ono T and Esashi M 2005 Effect of ion attachment on mechanical dissipation of a resonator *Appl. Phys. Lett.* **87** 044105

[170] Naik A K *et al* 2009 Towards single-molecule nanomechanical mass spectrometry *Nat. Nanotechnol.* **4** 445–50

[171] Hanay M S *et al* 2012 Single protein nanomechanical mass spectrometry in real time *Nat. Nanotechnol.* **7** 602–8

[172] Park J *et al* 2011 A mechanical nanomembrane detector for time-of-flight mass spectrometry *Nano Lett.* **11** 3681–4

[173] Park J, Kim H and Blick R H 2012 Quasi-dynamic mode of nanomembranes for time-of-flight mass spectrometry of proteins *Nanoscale* **4** 2543–8

[174] Park J and Blick R H 2013 A silicon nanomembrane detector for matrix-assisted laser desorption/ionization time-of-flight mass spectrometry (MALDI-TOF MS) of large proteins *Sensors* **13** 13708–16

[175] Eaton W P and Smith J H 1997 Micromachined pressure sensors: review and recent developments *Smart Mater. Struct.* **6** 530–9

[176] Catling D C 1998 High-sensitivity silicon capacitive sensors for measuring medium-vacuum gas pressures *Sensors Actuators* A **64** 157–64

[177] Esashi M *et al* 1998 Vacuum-sealed silicon micromachined pressure sensors *Proc. IEEE* **86** 1627–39

[178] Kurth S *et al* 2002 A new vacuum friction gauge based on a Si tuning fork *Sensors Actuators* A **97–98** 167–72

[179] Tenholte D *et al* 2008 A MEMS friction vacuum gauge suitable for high temperature environment *Sensors Actuators* A **142** 166–72

[180] van Herwaarden A W, Sarro P M and Meiher H C 1985 Integrated vacuum sensor *Sensors Actuators* **8** 187–96

[181] van Herwaarden A W and Sarro P M 1988 Performance of integrated thermopile vacuum sensors *J. Phys. E. Sci. Instrum.* **21** 1162–7

[182] Weng P K and Shie J-S 1994 Micro-Pirani vacuum gauge *Rev. Sci. Instrum.* **65** 492–9

[183] Ruellan J *et al* 2013 Pirani gauge based on alternative self-heating of silicon nanowire *Proc. Transducers Conf. (Barcelona, Spain, 16–20 June 2013)* pp 2568–71

[184] Zhang F T *et al* 2006 A micro-Pirani vacuum gauge based on micro-hotplate technology *Sensors Actuators* A **126** 300–5

[185] Mastrangelo C H and Muller R S 1991 Microfabricated thermal absolute-pressure sensor with on-chip digital front-end processor *IEEE J. Solid-State Circuits* **26** 1998–2007

[186] Paul O and Baltes H 1995 Novel fully CMOS-compatible vacuum sensor *Sensors Actuators* A **46** 143–6

[187] Klaassen E H and Kovacs G T A 1997 Integrated thermal-conductivity vacuum sensors *Sensors Actuators* A **58** 37–42

[188] 925 Micropirani™ vacuum transducer (www.mksinstr.com)

[189] Jousten K (ed) 2008 *Handbook of Vacuum Technology* (Weinheim: Wiley-VCH)

[190] Kline-Schoder R J and Sorensen P H 2007 Miniature high vacuum pump for analytical instruments *Proc. American Vacuum Society Conf.* (*Seattle, Washington, 14–19 October 2007*)

[191] Minivac (www.creare.com)

[192] Laser D J and Santiago J G 2004 A review of micropumps *J. Micromech. Microeng.* **14** R35–64

[193] Sugiyama K, Ukita Y and Takamura Y 2012 Development of on-chip vacuum generation by gas-liquid phase transition *Sensors Actuators* A **176** 138–42

[194] McNamara S and Gianchandani Y B 2005 On-chip vacuum generated by a micromachined Knudsen pump *J. Microelectromech. Syst.* **14** 741–6

[195] Gupta N K, An S, Gianchandani Y B 2012 A Si-micromachined 48-stage Knudsen pump for on-chip vacuum *J. Micromech. Microeng.* **22** 105026

[196] An S, Gupta N K and Gianchandani Y B 2014 A Si-micromachined 162-stage two-part Knudsen pump for on-chip vacuum *J. Microelectromech. Syst.* **23** 406–16

[197] Wright S A and Gianchandani Y B 2007 Controlling pressure in microsystem packages by on-chip microdischarges between thin-film titanium electrodes *J. Vac. Sci. Technol.* B **25** 1711–20

[198] Green S R, Malhotra R and Gianchandani Y B 2013 Sub-Torr chip-scale sputter-ion pump based on a Penning cell array architecture *J. Microelectromech. Syst.* **22** 309–17

[199] Koops H W P 2005 Proposal of a miniaturized orbitron vacuum pump for MEMS applications *Proc. SPIE* **5838** 38–42

[200] Doms M and Müller J 2005 A micromachined vapor jet pump *Sensors Actuators* A **119** 462–7

[201] Doms M and Müller J 2007 Design, fabrication, and characterization of a micro vapor-jet vacuum pump *J. Fluids. Eng.* **129** 1339–45

[202] Zhou H *et al* 2011 A single-stage micromachined vacuum pump achieving 164 Torr absolute pressure *Proc. IEEE MEMS Conf. (Cancun, Mexico, 23–27 January 2011)* pp 1095–8

[203] Kim H T, Park J W and Kim H 2011 All-electric peristaltic vacuum pump utilizing electro-magnetic and hydraulic actuation with a highly flexible latex membrane *Proc. Transducers Conf. (Beijing, People's Republic of China, 5–9 June 2011)* pp 2454–7

[204] Waits C M, McCarthy M and Ghodssi R 2010 A microfabricated spiral-groove turbopump supported on microball bearings *J. Microelectromech. Syst.* **19** 99–108

[205] Gannon A J *et al* 2014 MEMS-scale turbomachinery based vacuum roughing pump *J. Turbomach.* **136** 101002

[206] Yang W and Gu A 2012 Radial turbomolecular pump with electrostatically levitated rotor *US Patent Specification* 8221098

[207] Malcolm A *et al* 2010 Miniature mass spectrometer systems based on a microengineered quadrupole filter *Anal. Chem.* **82** 1751–8

[208] Isolera Dalton (www.biotage.com)

[209] Wright S *et al* 2015 A microelectromechanical systems-enabled, miniature triple quadrupole mass spectrometer *Anal. Chem.* **87** 3115–22

[210] Hauschild J-P, Wapelhorst E and Müller J 2007 Mass spectra measured by a fully integrated MEMS mass spectrometer *Int. J. Mass Spectrom.* **264** 53–60

[211] Hauschild J-P, Wapelhorst E and Müller J 2009 The novel synchronous ion shield mass analyzer *J. Mass Spectrom.* **44** 1330–7

[212] Reinhardt M *et al* 2010 Helium detection using a planar integrated micro-mass spectrometer *Int. J. Mass Spectrom.* **295** 145–8

[213] McFadden W H 1973 *Techniques of Combined Gas Chromatography/Mass Spectrometry: Applications in Organic Analysis* (New York: Wiley)

[214] Eiceman G A, Karpas Z and Hill H H 2013 *Ion Mobility Spectrometry* 3rd edn (Boca Raton, FL: CRC Press)

[215] Niessen W M A 2006 *Liquid Chromatography—Mass Spectrometry* (New York: Marcel Dekker)

[216] Landers J P 2007 *Handbook of Capillary and Microchip Electrophoresis and Associated Microtechniques* 3rd edn (Boca Raton, FL: CRC Press)

[217] Terry S C, Jerman J H and Angell J B 1979 A gas chromatographic air analyzer fabricated on a silicon wafer *IEEE Trans. Electron Devices* **26** 1880–6

[218] Noh H, Hesketh P J and Frye-Mason G C 2002 Parylene gas chromatographic column for rapid thermal cycling *J. Microelectromech. Syst.* **11** 718–25

[219] Agah M and Wise K D 2007 Low-mass PECVD oxynitride gas chromatographic columns *J. Microelectromech. Syst.* **16** 853–60

[220] Bhushan A *et al* 2007 Fabrication and preliminary results for LiGA fabricated nickel micro gas chromatography columns *J. Microelectromech. Syst.* **16** 383–93

[221] Lehmann U *et al* 2000 Micromachined gas chromatograph based on a plasma polymerised stationary phase *Proc. µTAS Conf. (Enschede, The Netherlands, 14–18 May 2000)* pp 167–70

[222] Nakai T *et al* 2009 Micro-fabricated semi-packed column for gas chromatography by using functionalized parylene as a stationary phase *J. Micromech. Microeng.* **19** 065032

[223] Zareian-Jahromi M A and Agah M 2010 Microfabricated gas chromatography columns with monolayer-protected gold stationary phases *J. Microelectromech. Syst.* **19** 294–304

[224] Shakeel H, Rice G W and Agah M 2014 Semipacked columns with atomic layer-deposited alumina as a stationary phase *Sensors Actuators* B **203** 641–6

[225] Zareian-Jahromi M A *et al* 2009 Design, modeling and fabrication of MEMS-based multicapillary gas chromatographic columns *J. Microelectromech. Syst.* **18** 28–37

[226] Nachef K *et al* 2012 Micro gas chromatography sample injector for the analysis of natural gas *J. Microelectromech. Syst.* **21** 730–8

[227] Agah M *et al* 2005 High-performance temperature-programmed microfabricated gas chromatography columns *J. Microelectromech. Syst.* **14** 1039–50

[228] Qin Y and Gianchandani Y B 2014 iGC2: an architecture for micro gas chromatographs utilizing integrated bi-directional pumps and multi-stage preconcentrators *J. Micromech. Microeng.* **24** 065011

[229] Akbar M, Shakeel H and Agah M 2015 GC-on-chip: integrated column and photoionization detector *Lab Chip* **15** 1748–58

[230] Lu C-J *et al* 2003 Portable gas chromatograph with tunable retention and sensor array detection for the determination of complex vapor mixtures *Anal. Chem.* **75** 1400–9

[231] Dziubian J A *et al* 2004 Portable gas chromatograph with integrated components *Sensors Actuators* A **115** 318–30

[232] Holland P M *et al* 2003 Miniaturized GC/MS instrumentation for *in situ* measurements: micro gas chromatography coupled with miniature quadrupole array and Paul ion trap mass spectrometers *Proc. SPIE* **4878** 1–7

[233] Diaz J A *et al* 2004 Integration test of a miniature $E \times B$ mass spectrometer with a gas chromatograph for development of a low-cost, portable, chemical detection system *Trends Anal. Chem.* **23** 314–21

[234] Miller R A *et al* 2000 A novel micromachined high-field asymmetric waveform-ion mobility spectrometer *Sensors Actuators* B **67** 300–6

[235] Davis C E *et al* 2003 Spore biomarker detection using a MEMS differential mobility spectrometer *Proc. Transducers Conf. (Boston, MA, 8–12 June 2003)* pp 1233–8

[236] Shvartsburg A A *et al* 2006 High-resolution field asymmetric waveform ion mobility spectrometry using new planar geometry analyzers *Anal. Chem.* **78** 3706–14

[237] Eiceman G A *et al* 2007 Planar drift tube for ion mobility spectrometry *Instrum. Sci. Technol.* **35** 365–83

[238] Shvartsburg A A *et al* 2009 Ultrafast differential ion mobility spectrometry at extreme electric fields in multichannel microchips *Anal. Chem.* **81** 6489–95

[239] Schvartsburg A A and Smith R D 2012 Protein analyses using differential ion mobility microchips with mass spectrometry *Anal. Chem.* **84** 7297–300

[240] Lonestar Portable Analyzer (www.owlstonenanotech.com)

[241] Ohla S and Belder D 2012 Chip-based separation devices coupled to mass spectrometry *Curr. Opin. Chem. Biol.* **16** 453–9

[242] Lin S L, Lin T Y and Fuh M R 2013 Recent developments in microfluidic chip-based separation devices coupled to MS for bioanalysis *Bioanalysis* **5** 2567–80

[243] Oedit A *et al* 2015 Lab-on-a-chip hyphenation with mass spectrometry: strategies for bioanalytical applications *Curr. Opin. Biotechnol.* **31** 79–85

[244] Manz A *et al* 1990 Design of an open-tubular column liquid chromatograph using silicon chip technology *Sensors Actuators* B **1** 249–55

[245] Ocvirk G *et al* 1995 High performance liquid chromatography partially integrated onto a silicon chip *Anal. Methods Instrum.* **2** 74–82

[246] Shih C-Y *et al* 2006 On-chip temperature gradient interaction chromatography *J. Chromatogr.* A **1111** 272–8

[247] Xie J *et al* 2005 Microfluidic platform for liquid chromatography-tandem mass spectrometry analyses of complex peptide mixtures *Anal. Chem.* **77** 6947–53

[248] Fuentes H V and Woolley A T 2007 Electrically actuated, pressure-driven liquid chromatography separations in microfabricated devices *Lab Chip* **7** 1524–31

[249] Yang Y and Chae J 2008 Miniaturized protein separation using a liquid chromatography column on a flexible substrate *J. Micromech. Microeng.* **18** 125010

[250] Ehlert S *et al* 2008 Separation efficiency of particle-packed HPLC microchips *Anal. Chem.* **80** 5945–50

[251] Song Y *et al* 2012 Integration of pillar array columns into a gradient elution system for pressure-driven liquid chromatography *Anal Chem.* **84** 4739–45

[252] Lazar I M and Kabulski J L 2013 Microfluidic LC device with orthogonal sample extraction for on-chip MALDI-MS detection *Lab Chip* **13** 2055–65

[253] Yin H *et al* 2005 Microfluidic chip for peptide analysis with an integrated HPLC column, sample enrichment column, and nanoelectrospray tip *Anal. Chem.* **77** 527–33

[254] Yin H and Killeen K 2007 The fundamental aspects and applications of Agilent HPLC-chip *J. Sep. Science* **30** 1427–34

[255] Carlier J *et al* 2005 Integrated microfabricated systems including a purification module and an on-chip nano electrospray ionization interface for biological analysis *J. Chromatogr.* A **1071** 213–22

[256] Liu J *et al* 2007 Monolithic column plastic microfluidic device for peptide analysis using electrospray from a channel opening on the edge of the device *Int. J. Mass Spectrom.* **259** 65–72

[257] Mery E *et al* 2008 A silicon microfluidic chip integrating an ordered micropillar array separation column and a nano-electrospray emitter for LC/MS analysis of peptides *Sensors Actuators* B **134** 438–46

[258] Sainiemi L *et al* 2012 A microfabricated micropillar liquid chromatographic chip monolithically integrated with an electrospray ionization tip *Lab Chip* **12** 325–32

[259] Harrison D J *et al* 1992 Capillary electrophoresis and sample injection systems integrated on a planar glass chip *Anal. Chem.* **64** 1926–32

[260] McCormick R M *et al* 1997 Microchannel electrophoretic separations of DNA in injection-molded plastic substrates *Anal. Chem.* **69** 2626–30

[261] Lin Y-C *et al* 2001 A poly-methylmethacrylate electrophoresis microchip with sample preconcentrator *J. Micromech. Microeng.* **11** 189–94

[262] Chen X *et al* 2002 A prototype 2D capillary electrophoresis system fabricated in poly(dimethylsiloxane) *Anal. Chem.* **74** 1772–8

[263] Zhang B *et al* 1999 Microfabricated devices for capillary electrophoresis-electrospray mass spectrometry *Anal. Chem.* **71** 3258–64

[264] Wen J *et al* 2000 Microfabricated isoelectric focusing device for direct electrospray-ionization mass spectrometry *Electrophoresis* **21** 191–7

[265] Dahlin A P *et al* 2005 Poly(dimethylsiloxane)-based microchip for 2D solid-phase extraction-capillary electrophoresis with an integrated electrospray emitter tip *Anal. Chem.* **77** 5356–63

[266] Sikanen T *et al* 2007 Fully microfabricated and integrated SU-8-based capillary electrophoresis-electrospray ionization microchips for mass spectrometry *Anal. Chem.* **79** 9135–44

[267] Nordman N *et al* 2011 Rapid and sensitive drug metabolism studies by SU-8 microchip capillary electrophoresis-electrospray ionization mass spectrometry *J. Chromatogr.* A **1218** 739–45

[268] Sikanen T *et al* 2012 Microchip capillary electrophoresis-electrospray ionization mass spectrometry of intact proteins using uncoated Ormocomp microchips *Anal. Chim. Acta* **711** 69–76

[269] Lazar I M *et al* 2003 Microfluidic device for capillary electro-chromatography-mass spectrometry *Electrophoresis* **24** 3655–62

[270] He M *et al* 2015 Development and characterizations of a miniature capillary electrophoresis mass spectrometry system *Anal. Chem.* **87** 2236–41

[271] Patterson G E *et al* 2002 Miniature cylindrical ion trap mass spectrometer *Anal. Chem.* **74** 6145–53

[272] Gao L *et al* 2006 Handheld rectilinear ion trap mass spectrometer *Anal. Chem.* **78** 5994–6002

[273] Li L *et al* 2014 Mini 12, miniature mass spectrometer for clinical and other applications—introduction and characterization *Anal. Chem.* **86** 2909–16

[274] Griffin 460 (www.flir.com)

[275] M908 (http://908devices.com)

[276] Yang M *et al* 2008 Development of a palm portable mass spectrometer *J. Am. Soc. Mass Spectrom.* **19** 1442–8

[277] Contreras J A *et al* 2008 Hand-portable gas chromatograph-toroidal ion trap mass spectrometer (GC-TMS) for detection of hazardous compounds *J. Am. Soc. Mass Spectrom.* **19** 1425–34

[278] Tridion-9 (http://torion.com)

[279] Guardion (www.smithsdetection.com)

[280] Finlay A *et al* 2006 Microsaic Ionchip: the first commercially available mass spectrometer chip *Proc. Pittcon Conf. (Orlando, FL, 12–17 March 2006)* paper 681-1

[281] Moore D S 2004 Instrumentation for trace detection of high explosives *Rev. Sci. Instrum.* **75** 2499–512

[282] Takáts T *et al* 2005 Direct, trace-level detection of explosives on ambient surfaces by desorption electrospray ionization mass spectrometry *Chem. Commun.* **15** 1950–2

[283] Sanders N L *et al* 2010 Detection of explosives as negative ions directly from surfaces using a miniature mass spectrometer *Anal. Chem.* **82** 5313–6

[284] Chen W *et al* 2013 Non-contact halogen lamp heating assisted LTP ionization miniature rectilinear ion trap: a platform for rapid, on-site explosives analysis *Analyst* **138** 5068–73

[285] McGill R A *et al* 2000 The design of functionalized silicone polymers for chemical sensor detection of nitroaromatic compounds *Sensors Actuators* B **65** 5–9

[286] Lima R R *et al* 2005 Production and deposition of adsorbent films by plasma polymerization on low cost micromachined non-planar microchannels for preconcentration of organic compound in air *Sensors Actuators* B **108** 435–44

[287] Manginell R P *et al* 2000 Microfabricated planar preconcentrator *Proc. Solid State Sensor and Actuator Workshop (Hilton Head, SC, 4–8 June 2000)* pp 179–82

[288] Kim M and Mitra S 2003 A microfabricated microconcentrator for sensors and gas chromatography *J. Chromatogr.* A **996** 1–11

[289] Tian W-C *et al* 2003 Microfabricated preconcentrator-focuser for a microscale gas chromatograph *J. Microelectromech. Syst.* **12** 264–72

[290] Bae B *et al* 2007 A five-valve fully integrated preconcentrator *Proc. IEEE Sensors Conf. (Atlanta, GA, 28–32 October 2007)* pp 1353–6

[291] Baker C *et al* 2009 Monolithic MEMS vacuum valves for miniature chemical pre-concentrators *Proc. Transducers Conf. (Denver, CO, 21–25 June 2009)* pp 1826–9

[292] McGill R A *et al* 2003 A micromachined preconcentrator for enhanced trace detection of illicit materials *Proc. Semiconductor Device Research Symp. (10–12 December 2003)* p 494

[293] Pai R S *et al* 2007 Towards enhanced detection of chemical agents: design and development of a microfabricated preconcentrator *Proc. Transducers Conf. (Lyon, France, 10–14 June 2007)* pp 2291–4

[294] Aebersold J *et al* 2008 Microfabrication process and characteristic testing of a MEMS-based preconcentrator *Proc. Bienniel UGIM Micro/Nano Symp. (Louisville, KY, 13–16 July 2008)* pp 61–3

[295] Martin M D *et al* 2010 Performance of stacked, flow-through micropreconcentrators for portable trace detection *Int. J. Ion Mobil. Spectrom.* **13** 109–19

[296] Kientz C E 1998 Chromatography and mass spectrometry of chemical warfare agents, toxins and related compounds: state of the art and future prospects *J. Chromatogr.* A **814** 1–23

[297] Smith P A *et al* 2004 Detection of gas-phase chemical warfare agents using field-portable gas chromatography-mass spectrometry systems: instrument and sampling strategy considerations *Trends Anal. Chem.* **23** 296–306

[298] Diken E G *et al* 2012 Advances in field-portable ion trap GC/MS instrumentation *Proc. SPIE* **8358** 83581H

[299] Progent F *et al* 2013 Development of a micro-GC/Micro-mass-spectrometer for chemical threat *in situ* detection *Proc. Int. Symp on Protection against Chemical and Biological Warfare Agents (Stockholm, Sweden, 3–5 June 2013)*

[300] Rodriguez-Cruz S E 2006 Rapid analysis of controlled substances using desorption electrospray ionization mass spectrometry *Rapid Commun. Mass Spectrom.* **20** 53–60

[301] Kirby A E *et al* 2014 Analysis on the go: quantitation of drugs of abuse in dried urine with digital microfluidics and miniature mass spectrometry *Anal. Chem.* **86** 6121–9

[302] Eckenrode B A 2001 Environmental and forensic applications of field-portable GC-MS: an overview *J. Am. Soc. Mass. Spectrom.* **12** 683–93

[303] Ifa D R *et al* 2009 Forensic applications of ambient ionization mass spectrometry *Anal. Bioanal. Chem.* **394** 1995–2008

[304] Nier A O *et al* 1947 Mass spectrometer for leak detection *J. Appl. Phys.* **18** 30–3

[305] Pavalova A and Papazova D 2003 Oil-spill identification by gas chromatography-mass spectrometry *J. Chromatogr. Sci.* **41** 271–3

[306] Holowenko F M, MacKinnon M D and Fedorak P M 2002 Characterization of napthenic acids in oil sands wastewaters by gas chromatography-mass spectrometry *Water Res.* **36** 2843–55

[307] Freifeld B M and Trautz R C 2006 Real-time quadrupole mass spectrometer analysis of gas in borehole fluid samples acquired using the U-tube sampling methodology *Geofluids* **6** 217–24

[308] Brkic B, France N and Taylor S 2011 Oil-in-water monitoring using membrane inlet mass spectrometry *Anal. Chem.* **83** 6230–6

[309] Mullins O C *et al* 2014 Downhole fluid analysis and asphaltene science for petroleum reservoir evaluation *Annu. Rev. Chem. Biomol. Eng.* **5** 325–45

[310] MMS-1000 (http://1stdetect.com)

[311] Expression CMS (www.advion.com)

[312] Hamilton S E *et al* 2014 Use of a miniature mass spectrometer to support pharmaceutical process chemistry *Org. Process Res. Dev.* **18** 103–8

[313] Browne D L *et al* 2012 Continuous flow reaction monitoring using an on-line miniature mass spectrometer *Rapid Commun. Mass Spectrom.* **26** 1999–2010

[314] Bristow T W T *et al* 2014 On-line monitoring of continuous-flow chemical synthesis using a portable, small footprint mass spectrometer *J. Am. Soc. Mass Spectrom.* **25** 1794–802

[315] Sodal I E *et al* 1972 A high performance miniature mass spectrometer for respiratory gas analysis *Biomed. Sci. Instrum.* **9** 21–4

[316] Turner P G *et al* 2008 Portable mass spectrometry for measurement of anaesthetic agents and methane in respiratory gases *Veterinary J.* **177** 36–44

[317] Gothard J W *et al* 1980 Applications of respiratory mass spectrometry to intensive care *Anaesthesia* **35** 890–5

[318] Philips M *et al* 2003 Detection of lung cancer with volatile markers in the breath *Chest* **123** 2115–23

[319] Balog J *et al* 2013 Intraoperative tissue identification using rapid evaporative ionization mass spectrometry *Sci. Transl. Med.* **5** 194ra93

[320] Kerian K S *et al* 2015 Differentiation of prostate cancer from normal tissue in radical prostatectomy specimens by desorption electrospray ionization and touch spray ionization mass spectrometry *Analyst* **140** 1090–8

[321] Chen C-H *et al* 2013 Development of a mass spectrometry sampling probe for chemical analysis in surgical and endoscopic procedures *Anal. Chem.* **85** 11843–50

[322] Jarmusch A K *et al* 2014 Detection of strep throat causing bacterium directly from medical swabs by touch spray-mass spectrometry *Analyst* **139** 4785–9

[323] Mulligan C C *et al* 2006 Direct monitoring of toxic compounds in air using a portable mass spectrometer *Analyst* **131** 556–7

[324] Keil A *et al* 2008 Monitoring of toxic compounds in air using a handheld rectilinear ion trap mass spectrometer *Anal. Chem.* **80** 734–41

[325] Smith J N *et al* 2010 Facility monitoring of toxic industrial compounds in air using an automated, fieldable, miniature mass spectrometer *Analyst* **135** 994–1003

[326] Hendricks P I *et al* 2014 Autonomous *in situ* analysis and real-time chemical detection using a backpack miniature mass spectrometer: concept, instrumentation development and performance *Anal. Chem.* **86** 2900–8

[327] Bell R J *et al* 2007 Calibration of an *in situ* membrane inlet mass spectrometer for measurement of dissolved gases and volatile organics in seawater *Environ. Sci. Technol.* **41** 8123–8

[328] Hemond H F, Mueller A V and Hemond M 2008 Field testing of lake water chemistry with a portable and an AUV-based mass spectrometer *J. Am. Soc. Mass Spectrom.* **19** 1403–10

[329] Griffin T P *et al* 2008 3D concentration mapping of gases using a portable mass spectrometer *J. Am. Soc. Mass Spectrom.* **19** 1411–8

[330] Diaz J A *et al* 2010 Utilization of *in situ* airborne MS-based instrumentation for the study of gaseous emissions at active volcanoes *Int. J. Mass Spectrom.* **295** 105–12

[331] Ren X-X *et al* 2013 Rapid and direct analysis of active ingredients in drug tablets using atmospheric pressure laser desorption ionization mass spectrometry *Chin. J. Anal. Chem.* **41** 366–70

[332] Malik A K, Blasco C and Picó Y 2010 Liquid chromatography-mass spectrometry in food safety *J. Chromatogr.* A **1217** 4018–40

[333] Chu X *et al* 2011 China's food safety regulation and mass spectrometry *Methods Mol. Biol.* **747** 21–51

[334] Pei X *et al* 2011 The China melamine milk scandal and its implications for food safety regulation *Food Policy* **36** 412–20

[335] Dou H-L *et al* 2009 Determination of melamine in milk powder by GC/MS *J. Chin. Mass Spectrom. Soc.* **30** 167–9

[336] Huang G *et al* 2010 Direct analysis of melamine in complex matrices using a handheld mass spectrometer *Analyst* **135** 705–11

[337] Li L *et al* 2014 High efficiency tandem mass spectrometry analysis using dual linear ion traps *Analyst* **139** 4779–84

[338] Nier A O 1985 Mass spectrometry in planetary research *Int. J. Mass Spectrom. Ion Process.* **66** 55–73

[339] Palmer P T and Limero T F 2001 Mass spectrometry in the US Space Program: past, present and future *J. Am. Soc. Mass Spectrom.* **12** 656–75

[340] Hilchenbach H 2002 Space-borne mass spectrometer instrumentation *Int. J. Mass Spectrom.* **215** 113–29

[341] Hoffman J H, Chaney R C and Hammack H 2008 Phoenix Mars mission—the thermal evolved gas analyzer *J. Am. Soc. Mass Spectrom.* **19** 1377–83

[342] Rohner U *et al* 2004 Highly miniaturized laser ablation time-of-flight mass spectrometer for a planetary rover *Rev. Sci. Instrum.* **75** 1314–22

[343] Sinha M P *et al* 2011 Laser ablation-miniature mass spectrometer for elemental and isotopic analysis of rocks *Rev. Sci. Instrum.* **82** 094102

[344] Chutjian A *et al* 2000 A miniature quadrupole mass spectrometer array and GC for space flight: astronaut EVA and cabin-air monitoring *Int. Conf. on Environmental Systems (Toulouse, France)* SAE Technical paper 2000-01-2300

[345] Chaudhary A *et al* 2013 Micromachined mass spectrometer for low cost space missions *Proc. IAA Low-Cost Planetary Missions Conf. (Pasadena, CA, 18–20 June 2013)*

[346] Zheng Y *et al* 2015 MEMS fabrication of micro cylindrical ion trap (μCIT) mass spectrometer for CubeSats application *Eur. Planet. Sci. Abstr.* **10** EPCS2015-328

[347] Kielpinski D, Monroe C and Wineland D J 2002 Architecture for a large-scale ion-trap quantum computer *Nature* **417** 709–11

[348] Reichel J 2002 Microchip traps and Bose-Einstein condensation *Appl. Phys.* B **75** 469–87

[349] Chiaverini J *et al* 2005 Surface-electrode architecture for ion-trap quantum information processing *Quantum Inf. Comput.* **5** 419–39

[350] See P, Wilpers G, Gill P and Sinclair A G 2013 Fabrication of a monolithic array of 3D Si-based ion traps *J. Microelectromech. Syst.* **22** 1180–9

[351] Hensinger W K *et al* 2006 T-junction ion trap array for 2D ion shuttling, storage and manipulation *Appl. Phys. Lett.* **88** 034101

[352] Blakestad R B *et al* 2009 High-fidelity transport of trapped-ion qubits through an X-junction trap array *Phys. Rev. Lett.* **102** 153002

[353] Brama E *et al* 2012 Heating rates in a thin ion trap for microcavity experiments *Appl. Phys.* B **107** 945–54

[354] Sterling R C *et al* 2013 Increased surface flashover voltage in microfabricated devices *Appl. Phys. Lett.* **103** 143504

[355] Sterling R C *et al* 2014 Fabrication and operation of a 2D ion-trap lattice on a high-voltage microchip *Nat. Commun.* **5** 3637